Nuclear structure of ^{196}Au: More evidence for its supersymmetric description

J. Gröger,[1] J. Jolie,[2] R. Krücken,[3] C. W. Beausang,[3] M. Caprio,[3] R. F. Casten,[3] J. Cederkall,[3] J. R. Cooper,[3] F. Corminboeuf,[2] L. Genilloud,[2] G. Graw,[4] C. Günther,[1] M. de Huu,[2] A. I. Levon,[1,5] A. Metz,[4] J. R. Novak,[3] N. Warr,[2] and T. Wendel[1]

[1]*Institut für Strahlen- und Kernphysik, Universität Bonn, D-53115 Bonn, Germany*

[2]*Institut de Physique, Université de Fribourg, Perolles, CH-1700 Fribourg, Switzerland*

[3]*A.W. Wright Nuclear Structure Laboratory, Yale University, New Haven, Connecticut 06520*

[4]*Ludwig-Maximilian Universität, Am Coulombwall 1, D-85748 Garching, Germany*

[5]*Institute for Nuclear Research, 252028 Kiev, Ukraine*

(Received 26 May 2000; published 2 November 2000)

Excited states in ^{196}Au, populated in the ^{196}Pt(p,n) and $(d,2n)$ reactions, were investigated by in-beam γ-ray and conversion-electron spectroscopy. Two only weakly connected level structures, built on the 2^- ground state (negative-parity level scheme) and on the 5^+ isomer at 84.7 keV (positive-parity level scheme), are observed. The point of main effort of the present work was the investigation of the negative-parity level scheme in connection with its description within the framework of an extended supersymmetry. For this level scheme we observe 25 excited states up to an excitation energy of 500 keV, of which 23 had already been identified in a recent study of ^{196}Au by transfer reactions. From 500 to 800 keV we observe 28 additional levels compared to 20 levels observed in the transfer reactions. The excitation energies derived in the studies of the (p,n) compound reaction and the (p,d) transfer reaction agree within 1 keV, and the complementary information obtained from the two reactions led to improved spin determinations. The negative-parity level structure is compared with the predictions of the extended supersymmetry.

PACS number(s): 21.60.Fw, 23.20.−g, 25.40.−h, 27.80.+w

I. INTRODUCTION

Since its introduction 25 years ago the interacting boson model (IBM) has been remarkably successful in the description of the nuclear structure of heavy nuclei. This model was originally developed for nuclei with an even number of protons and neutrons (even-even nuclei) which are assumed to couple to pairs behaving approximately as bosons [1]. The level structure of even-even nuclei can then be described by such interacting bosons. This model was soon extended to nuclei with an odd number of nucleons (odd-*A* nuclei) leading to a model of interacting bosons and fermions (IBFM). In 1980 Iachello developed a supersymmetric theory in which bosonic and fermionic levels are combined in common multiplets [2]. This theory leads to relations between odd-*A* nuclei and their even-even core nuclei which were found to be realized in several pairs of nuclei, providing firm evidence for this aspect of nuclear supersymmetry. As a logical final step it was proposed that this theory could be extended to odd-odd nuclei [3,4]. A theoretical formalism of ''quartet supersymmetry'' was developed in which the properties of a quartet of nuclei with equal number of bosons plus fermions could be linked by supersymmetry. The test of such a scheme requires detailed experimental information on the spectroscopic properties of the odd-odd member of the quartet. Due to the extremely complex structure of odd-odd nuclei such information was not available until recently, and therefore the realization of the extended supersymmetry in nuclei was not convincingly demonstrated.

It was realized early that the best candidate for a test of the extended supersymmetry is the quartet of nuclei consisting of ^{194}Pt, ^{195}Pt, ^{195}Au, and ^{196}Au [3,5]. In these nuclei the unpaired proton occupies an isolated $2d_{3/2}$ orbital and the unpaired neutron the $3p_{1/2}$, $3p_{3/2}$, and $2f_{5/2}$ members of a subshell. The even-even member of the quartet ^{194}Pt is known to exhibit the $O(6)$ symmetry of the IBM. It is then possible to predict the low-lying levels with negative parity in ^{196}Au by applying supersymmetric transformations to the experimentally known energy spectra of ^{194}Pt, ^{195}Pt, and ^{195}Au. Such a prediction, involving only six phenomenological parameters, has been given by Jolie *et al.* [5]. Unfortunately, the information on the structure of ^{196}Au from earlier experimental work [5,6] was too incomplete to allow a meaningful comparison with the calculated spectra. We have therefore started a new experimental program to investigate the level structure of ^{196}Au. High resolution transfer experiments with protons and polarized deuterons were performed at the tandem accelerator of the TU/LMU München. These experiments led to a level scheme for the negative parity levels of ^{196}Au which provided the first solid evidence for the existence of the extended supersymmetry in nuclei [7,8]. Simultaneously, an investigation of the decay of the ^{196}Au compound nucleus, populated in the (p,n) and $(d,2n)$ reactions on ^{196}Pt targets, by in-beam gamma ray and conversion electron spectroscopy was started. These latter investigations are reported in the present paper, and the results are compared with those of the transfer experiments and with the theoretical predictions.

II. EXPERIMENTAL METHODS AND RESULTS

The ^{196}Pt$(p,n)^{196}$Au reaction is expected to dominate at proton bombarding energies below 10 MeV, as compared to the Coulomb barrier for this reaction of $\sim$13 MeV. We therefore chose for our first measurements the $(d,2n)$ reaction. Gamma-gamma coincidences were measured at the cyclotron of the PSI (Villigen, Switzerland) using the setup described by Warr *et al.* [9], and conversion electrons and

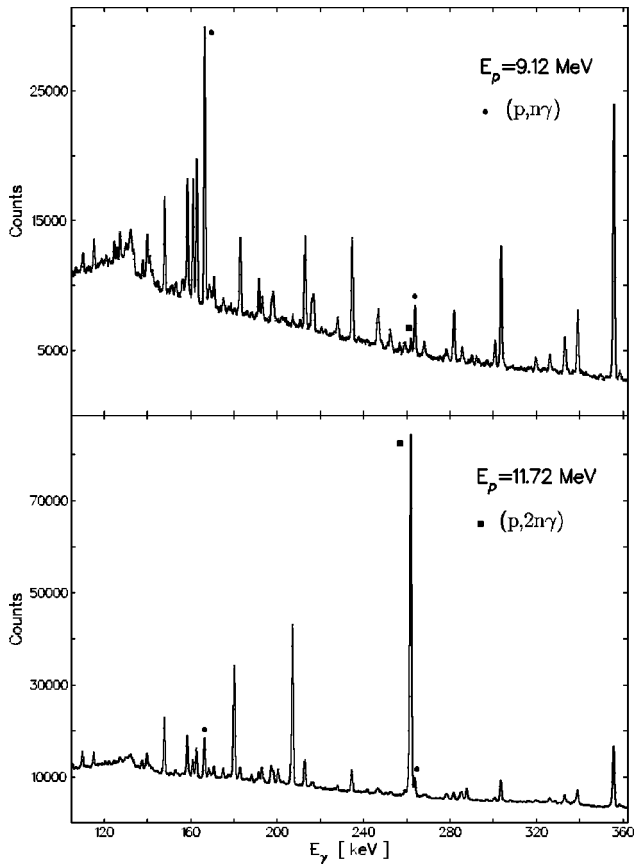

FIG. 1. Gamma-ray spectra obtained by bombarding a ^{196}Pt target with 9.1 and 11.7 MeV protons. The γ rays were detected using a LEPS detector with an energy resolution of 700 eV at 100 keV.

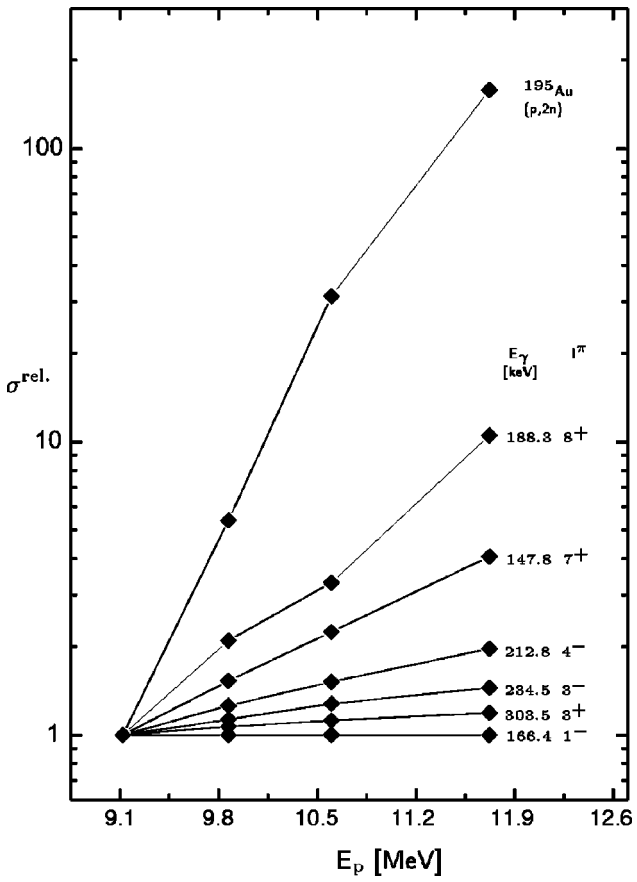

FIG. 2. Excitation functions for selected γ rays obtained in the ^{196}Pt(p,xn) reactions.

electron-gamma coincidences were measured at the cyclotron of the University of Bonn. These measurements led, together with the level structure of ^{196}Au known by then from the transfer reactions, to an identification of the strongest γ rays in ^{196}Au, and a preliminary decay scheme for its low-lying levels [10,11]. With this knowledge we performed a measurement of the excitation functions for the (p,xn) reactions which showed that the (p,n) reaction at $E_p \approx 9$ MeV is most favorable for the investigation of the low-spin level structure of ^{196}Au. In the following we will discuss the results obtained in this reaction apart from a few exceptions, where we used the $(d,2n)$ reaction because of its larger cross section and higher spin transfer.

A. Excitation functions

For the measurement of excitation functions a 10 mg/cm^2 thick metallic target enriched to 97.5% in ^{196}Pt was bombarded with protons of 9.1, 9.9, 10.6, and 11.7 MeV at the Bonn cyclotron. Singles γ-ray spectra were recorded with a LEPS detector placed at a backward angle of 55° with respect to the beam direction.

The γ-ray spectra obtained at the lowest and highest proton energy are shown in Fig. 1. The strongest γ ray in ^{195}Au populated in the $(p,2n)$ reaction is marked by a filled square. Two γ rays in ^{196}Au are marked by circles. The lower one at 166.4 keV is the strongest γ ray observed in the negative-parity part of the level scheme of ^{196}Au (see Fig. 12 below). At 9.1 MeV we observe a very clean γ-ray spectrum from the (p,n) reaction with only a few strong contaminating lines from ^{196}Pt populated in Coulomb excitation and in the decay of the 6.2d ground state of ^{196}Au (for example the very strong 355.7 keV γ ray from the $2^+ \rightarrow 0^+$ transition seen at the upper end of Fig. 1). For the (p,n) cross section we obtain a rough estimate of 30 mb.

Excitation function curves for a few transitions, normalized at 9.1 MeV and to the 166.4 keV γ ray, are shown in Fig. 2. The assignments of these transitions, and their γ-ray intensities at 9.1 MeV bombarding energy, are given in Table I. The excitation curves show the characteristic dependence of the slope on the spin of the populated level, which is often used for spin determinations. Unfortunately, in the present case this technique can only be used for a few strongly populated levels since most observed γ rays are multiply assigned in the level scheme.

A complete list of the energies and intensities of all γ rays observed at the four proton bombarding energies is given in Ref. [13].

B. $\gamma\gamma$ coincidences

A first measurement of $\gamma\gamma$ coincidences following the (p,n) reaction was performed at the Bonn cyclotron with a

TABLE I. Assignments of the γ rays, for which excitation functions are shown in Fig. 2. The quoted γ-ray intensities are those measured in the bombardment of the ^{196}Pt target with 9.1 MeV protons.

Initial level E_{exc} [keV]	I^{π}	Final level E_{exc} [keV]	I^{π}	Transition E_{γ} [keV]	I_{γ}	Assignment
166.4	1^-	0.0	2^-	166.4	100	this work
212.8	4^-	0.0	2^-	212.8	43	this work
234.5	3^-	0.0	2^-	234.5	51	this work
388.2	3^+	84.7	5^+	303.5	90	this work
232.5	7^+	84.7	5^+	147.8	34	Ref. [12]
420.8	8^+	232.5	7^+	188.3	2	Ref. [12]
261.8	$5/2^+$	0.0	$3/2^+$	261.8	9	^{195}Au

coincidence setup containing five Compton-suppressed Ge detectors. Although this experiment already provided fairly detailed coincidence relations it also demonstrated that a measurement with a larger coincidence array was necessary to allow an interpretation of the very complex γ-ray spectrum with many weak and multiply assigned γ rays. A second $\gamma\gamma$-coincidence measurement was therefore carried out at the ESTU Tandem accelerator at Yale University, using the YRAST Ball γ-ray array [14]. This array was used in a configuration consisting of 4 four-element Clover detectors, 17 single-crystal HPGe detectors, and two LEPS detectors for the detection of low-energy γ rays. Most of the Clover and HPGe detectors were equipped with Compton suppression shields. The 10 mg/cm^2 ^{196}Pt target was bombarded with 9.1 MeV protons. A total of 6×10^8 coincidence events were accumulated during an effective time of data accumulation of 3 days and 4 h.

The data obtained with the YRAST Ball were sorted with appropriate time windows into different $4k\times4k$ matrices: 2.9×10^8 events into a Ge-Ge matrix, 4.5×10^7 events into a Ge-LEPS matrix and 5.3×10^6 events into a LEPS-LEPS matrix. These matrices were analyzed with the interactive RADWARE package [15].

As an illustration of the quality of our data and our reasoning for the assignment of the γ rays in the level scheme of ^{196}Au we show some sections of γ-ray spectra in Figs. 3–6. The spectra shown in Fig. 3 demonstrate the population and depopulation of a level at 234.5 keV. This level decays to the ground state and the first-excited state at 6.6 keV. This latter level was first observed in the recent transfer reaction experiments [7]. Our observation of the $\gamma\gamma$ coincidences shown in Fig. 3 provided the first firm evidence that we indeed observe γ rays belonging to ^{196}Au. In the subsequent analysis of the $\gamma\gamma$-coincidence data we identified the decay to the ground-state doublet for eight more levels.

The γ-ray spectra in coincidence with two transitions which populate a level at 258.6 keV are shown in Fig. 4. This level decays, in addition to its decay to the ground-state doublet (258.6 and 252.1 keV γ rays), to the second-excited level of ^{196}Au at 41.9 keV (216.7 keV γ ray). Both the 41.9 and 258.6 keV levels were identified in the transfer reactions with spin-parity assignments of 0^- and 4^-, respectively.

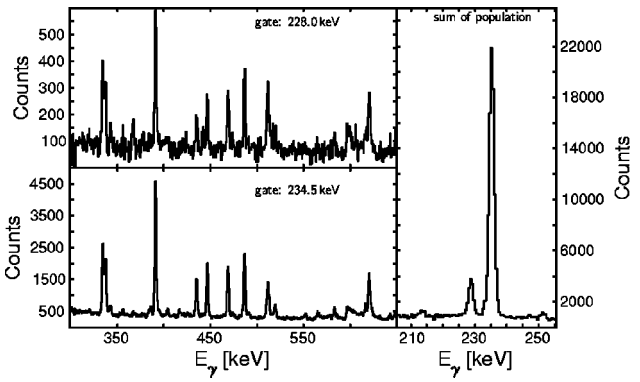

FIG. 3. Gamma-ray spectra in coincidence with γ rays populating (left) and depopulating (right) a level in ^{196}Au at 234.5 keV. In coincidence with depopulating γ rays one sees the populating spectrum and vice versa.

This example is one of the few cases where our data revise the spin-parity assignments derived previously from the transfer reaction experiments [7,8]. Since the parities of the two levels, as well as the 0^- assignment of the 41.9 keV level, seem safely established, the γ decay of the 258.6 keV level fixes its spin-parity to 1^- or 2^-.

The spectra shown in Fig. 4 also exemplify the problems encountered by double assignments of γ transitions. The 281.9 keV γ ray seen in the lower part of the figure results from the coincidence with a 557.9 keV γ ray populating a level at 323.8 keV, which is predominantly depopulated by the 281.9 keV γ ray. The 557.9 keV γ ray can of course not be resolved from the 557.4 keV γ ray populating the 258.6 keV level, but the two γ rays can be assigned unambiguously in the level scheme from the observed $\gamma\gamma$ coincidences. We might mention that we have identified yet an-

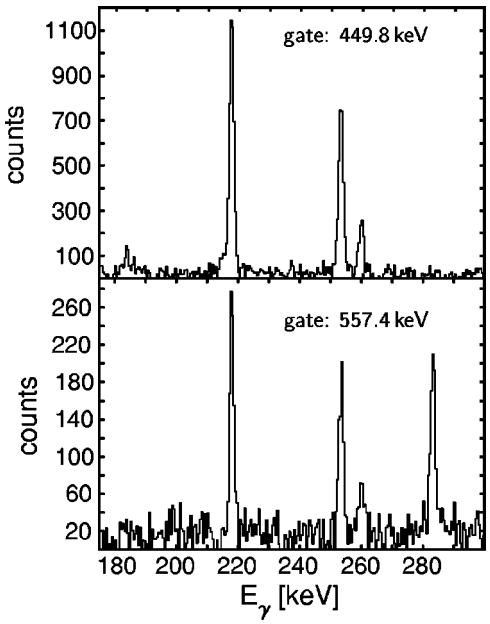

FIG. 4. Gamma-ray spectra in coincidence with γ rays populating a level in ^{196}Au at 258.6 keV (for the 282 keV line in the lower spectrum see text).

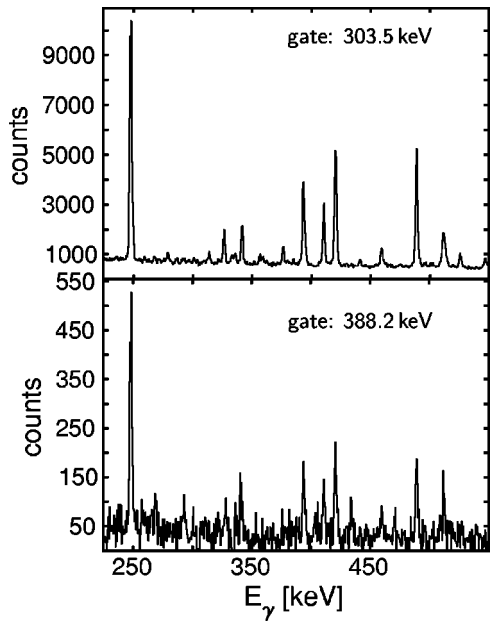

FIG. 5. Gamma-ray spectra in coincidence with γ rays depopulating a level in ^{196}Au at 388.2 keV.

other γ ray of 557.8 keV as a transition from a level at 720.4 keV to the 162.6 keV level.

In addition to the γ rays associated with the negative-parity levels we observe a second level structure, which at first seemed totally unconnected with the negative-parity structure. A careful analysis of the $\gamma\gamma$ coincidence data finally revealed a weak decay between these structures as shown in Fig. 5. A level at 388.2 keV decays by a strong 303.5 keV $E2$ transition to the known 5^+ isomer and two weak transitions to the 2^- ground state and the 4^- level at 212.8 keV (see Sec. III B).

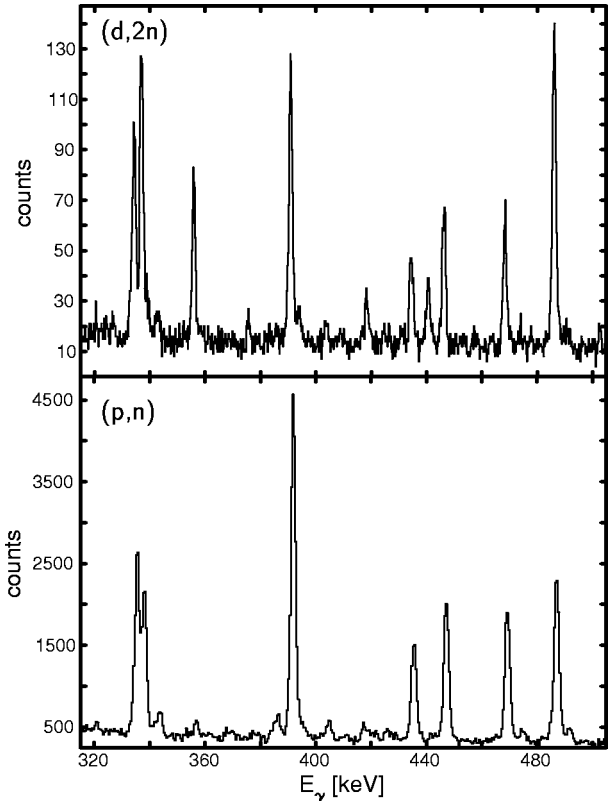

FIG. 6. Gamma-ray spectra in coincidence with the 234.5 keV transition in ^{196}Au, measured in the (p,n) and $(d,2n)$ reactions.

Finally, some information on the spins of the excited levels can be obtained from a comparison of the γ-ray spectra measured in the (p,n) and $(d,2n)$ reactions. As an example we show in Fig. 6 sections of the γ-ray spectra measured in coincidence with the 234.5 keV $3^-\rightarrow 2^-$ ground-state transition. The ratios $R=I_\gamma^{(d,2n)}/I_\gamma^{(p,n)}$ listed in Table II indicate that the 336.8 and 485.8 keV transitions depopulate levels with high spins. We tentatively assign $I^\pi=4^-$ to the 625.2 keV level (see Sec. II C) which suggests that the 571.5 and 720.4 keV levels have spin 5. Both levels decay to the 162.6 keV level which in turn decays to the 2^- ground state by a $M1$ transition restricting its spin to $\leqslant 3$. This latter level would then have $I^\pi=3^-$ contrary to the earlier 2^- assignment [7]. However, the 571.5 keV level decays most strongly by a 358.6 keV transition to the 212.8 keV 4^- level, and the 358.6–212.8 keV $\gamma\gamma$ angular correlation is only consistent with $I=4$ for this level (see Sec. II C). This shows that the conclusions drawn from the comparison of γ-ray intensities measured in the (p,n) and $(d,2n)$ reactions have to be taken with caution.

We have identified a total of approximately 110 levels in the level scheme built on the 2^- ground state, and approximately 90 levels built on the 5^+ isomer. Most of these levels are only identified in the $\gamma\gamma$ coincidences by depopulating γ rays. It is clear that we do not observe the transitions to the ground state, the two lowest excited levels at 6.5 and 41.9 keV and the 5^+ isomer at 84.7 keV for all those levels which are only populated by γ rays too weak to be observed with the $\gamma\gamma$ coincidence setup used in the present experiment. Consequently, we miss the levels which are only populated and depopulated by such γ rays.

In view of the complexity of the γ-ray spectrum with most γ rays being unresolved doublets or multiplets it is difficult to obtain reliable results for the intensities of the γ rays from the singles γ-ray spectrum, except for a few very strong γ rays (for example those listed in Table I). We therefore restrict our listing of γ-ray intensities to the negative-parity levels below 500 keV (Table III). These levels are of prime importance in connection with the supersymmetry scheme, and for most of them we also observe populating γ rays thus enabling the extraction of reasonably reliable γ-ray intensities from the $\gamma\gamma$ coincidence spectra. It should, however, be emphasized that the intensities listed in Table III were determined ignoring any effects from $\gamma\gamma$ angular cor-

TABLE II. Ratio of γ-ray intensities $R=I_\gamma^{(d,2n)}/I_\gamma^{(p,n)}$ of the γ rays shown in Fig. 6.

E_{exc} [keV]	568.7	571.5	625.2	668.8	680.5	702.6	720.4
E_γ [keV]	334.2	336.8	390.6	434.3	445.9	468.0	485.8
R	1.3	2.3	1.0	1.2	1.3	1.2	2.5

TABLE III. Gamma-ray branching ratios for the negative-parity levels in ^{196}Au up to 500 keV.

Transfer reactions [a]		$(p,n\gamma)$ reaction [b]						
Initial level		Initial level		Final level		Transition		
E_{exc}	I^{π}	E_{exc}	I^{π}	E_{exc}	I^{π}	E_{γ}	I_{γ}(rel.)	Multipolarity
162.4	$2^-,3^-$	162.6	$2^-,3^-$	0.0	2^-	162.6	100	$M1$
				6.6	1^-	156.1	$\leqslant 5$	
				41.9	0^-	120.7	$\leqslant 2$	
166.5	$1^-,2^-$	166.4	1^-	0.0	2^-	166.4	100	$M1$
				6.6	1^-	159.8	$\leqslant 1$	
				41.9	0^-	124.5	4.4	
		167.5	$1^-,2^-$	0.0	2^-	167.5	$\leqslant 10$	
				6.6	1^-	160.9	100	$M1$
				41.9	0^-	125.6	$\leqslant 6$	
197.8	$1^-,2^-$	198.0	$1^-,2^-$	0.0	2^-	198.0	44	
				6.6	1^-	191.5	100	
				41.9	0^-	156.4	20	
				166.4	1^-	31.6	6 [c]	$(M1)$
212.9	4^- [1^- to 4^-]	212.8	4^-	0.0	2^-	212.8	100	$E2$
				6.6	1^-	206.3	$\leqslant 1$	
				41.9	0^-	170.9	$\leqslant 1$	
				162.6	$2^-,3^-$	50.2	0.1 [c]	$(E2)$
233.5	$2^-,3^-,4^-$	234.5	3^-	0.0	2^-	234.5	100	$M1$
				6.6	1^-	228.0	18	
				41.9	0^-	192.7	$\leqslant 1$	
252.5	$1^-,2^-$	252.6	1^-	0.0	2^-	252.6	64	
				6.6	1^-	246.1	100	
				41.9	0^-	210.7	≈ 10	
				162.6	$2^-,3^-$	90.0	15	
				166.4	1^-	86.2	30	
				234.5	3^-	18.1	0.005 [c]	
257.9	1^- to 4^-	258.6	$1^-,2^-$	0.0	2^-	258.6	25	
				6.6	1^-	252.1	70	
				41.9	0^-	216.7	100	
				167.5	(1^-)	91.2		
287.4	$2^-,3^-$	288.2	2^-	0.0	2^-	288.2	$\leqslant 2$	
				6.6	1^-	281.6	100	$M1$
				41.9	0^-	246.2	19	
				162.6	$2^-,3^-$	125.5	$\leqslant 2$	
				166.4	1^-	121.8	$\leqslant 2$	
				167.5	(1^-)	120.6	5	
298.3	0^- to 3^-	298.5	$1^-,2^-$	0.0	2^-	298.4	≈ 20	
				6.6	1^-	292.1	100	
				41.9	0^-	256.6	71	
				166.4	1^-	132.2	42	
				167.5	(1^-)	131.2	≈ 15	
307.3	2^- [2^-]	307.3	2^-	0.0	2^-	307.2	$\leqslant 5$	
				6.6	1^-	300.7	100	
				41.9	0^-	258.8	$\leqslant 2$	
				162.6	$2^-,3^-$	144.5	$\leqslant 1$	
				166.4	1^-	140.8	$\leqslant 5$	
				167.5	(1^-)	139.7	15	
323.4	$1^-,2^-,3^-$	323.8	1^-	0.0	2^-	323.8	8	
				6.6	1^-	317.2	8	
				41.9	0^-	281.9	100	$M1$
				162.6	$2^-,3^-$	161.1	$\leqslant 6$	

TABLE III. (*Continued*).

Transfer reactions[a] Initial level		(p,n,γ) reaction[b] Initial level		Final level		Transition		
E_{exc}	I^π	E_{exc}	I^π	E_{exc}	I^π	E_γ	I_γ(rel.)	Multipolarity
				166.4	1^-	157.3	24	
				167.5	(1^-)	156.4	9	
				198.0	$1^-,2^-$	125.9	4	
				212.8	4^-	110.9	$\leqslant 3$	
		326.2	$1^-,2^-,3^-$	0.0	2^-	326.2	100	
				6.6	1^-	319.6	70	
				41.9	0^-	284.2	$\leqslant 3$	
				162.6	$2^-,3^-$	163.5	8	
				166.4	1^-	159.8	$\leqslant 2$	
				167.5	(1^-)	158.7	$\leqslant 2$	
				234.5	3^-	91.6		
348.1	$1^-,2^-$	349.2	2^-	0.0	2^-	349.2	13	
				6.6	1^-	342.8	19	
				41.9	0^-	307.3	$\leqslant 2$	
				162.6	$2^-,3^-$	186.5	$\leqslant 2$	
				166.4	1^-	182.8	100	$M1$
				167.5	(1^-)	181.7	≈ 8	
				198.0	$1^-,2^-$	151.2	≈ 4	
				212.8	4^-	136.3	$\leqslant 1$	
				234.5	3^-	114.6	≈ 2	$M1$
355.4	0^- to 3^-	355.9	(0^-)	258.6	$1^-,2^-$	97.3	100	
375.0	3^- $[2^-,3^-]$	375.7	3^-	0.0	2^-	375.7	100	
				167.5	(1^-)	208.3	6	
				212.9	4^-	162.7	16	$M1$
				234.5	3^-	141.0	2.9	
402.5	$2^-,3^-,4^-$	403.8	$3^-,4^-$	0.0	2^-	403.8	100	
				6.6	1^-	397.2	$\leqslant 2$	
				41.9	0^-	361.9	$\leqslant 2$	
				162.6	$2^-,3^-$	241.1	11	
				166.4	1^-	237.4	$\leqslant 1$	
				167.5	(1^-)	236.3	$\leqslant 1$	
				212.8	4^-	191.0	≈ 4	
				234.5	3^-	169.3	≈ 2	
407.4	$1^-,2^-,3^-$	408.4	0^- to 3^-	166.4	1^-	242.2	≈ 25	
				167.5	(1^-)	240.6	≈ 25	
				198.0	$1^-,2^-$	210.4	100	
				252.6	1^-	155.8		
				288.2	$1^-,2^-$	120.3	≈ 5	
413.0	2^- $[1^-,2^-]$	413.8	2^-	166.4	1^-	247.2	≈ 15	
				198.0	$1^-,2^-$	215.8	100	
				288.2	$1^-,2^-$	125.6	≈ 2	
				307.3	2^-	106.6		
455.6	2^- $[2^-]$	456.4[d]	2^-	162.6	$2^-,3^-$	293.8	$\leqslant 8$	
				166.4	1^-	290.0	100	
				167.5	(1^-)	289.0	34	
				234.5	3^-	221.7	8	
				252.6	1^-	203.8	49	
				258.6	$1^-,2^-$	197.8	41	
				323.8	1^-	132.7	≈ 10	
				349.3	2^-	107.5		

TABLE III. (*Continued*).

Transfer reactions[a] Initial level		(p,n,γ) reaction[b] Initial level		Final level		Transition		
E_{exc}	I^{π}	E_{exc}	I^{π}	E_{exc}	I^{π}	E_{γ}	I_{γ}(rel.)	Multipolarity
479.8	2^-	480.3	2^-	0.0	2^-	480.2	100	
				6.6	1^-	473.8	7	
				167.5	(1^-)	312.9	$\leqslant 3$	
				234.5	3^-	245.8	≈ 5	
				252.6	1^-	227.7	16	
				288.2	$1^-,2^-$	192.3	≈ 3	
				349.3	2^-	131.2	≈ 3	
				375.7	3^-	104.6		
490.6	3^-	490.2	3^-	0.0	2^-	490.2	100	
				6.6	1^-	483.7	9	
				41.9	0^-	448.3	$\leqslant 5$	
				162.6	$2^-,3^-$	327.7	≈ 13	
				166.4	1^-	323.7	≈ 15	
				167.5	(1^-)	322.7	≈ 15	
				234.5	3^-	255.7	$\leqslant 5$	
				252.6	1^-	237.6	20	
				288.2	$1^-,2^-$	202.0	18	
				307.3	2^-	183.2	$\leqslant 12$	
				349.3	2^-	141.0	20	
		491.4[d]	1^- to 4^-	198.0	$1^-,2^-$	293.3	100	

[a]Results from the transfer reaction experiments [7,8]. The excitation energies have errors of ± 0.6 keV. For discussions of the assigned spins see text.

[b]The energies and intensities have errors of ± 0.1 keV and $\pm 30\%$, respectively. The quoted multipolarities are dominant values derived in the conversion-electron measurements, and the spins are adopted values as discussed in Sec. III A.

[c]Estimated γ-ray intensities from total intensities assuming $M1$ multipolarity for the 31.6 keV transition and $E2$ multipolarity for the 18.1 and 50.3 keV transitions.

[d]No populating γ rays are observed for these levels. The listed γ-ray intensities are rough estimates derived from the $\gamma\gamma$ coincidence counting rates.

relations which are in general expected to be small (see Sec. II C).

One additional comment has to be made in connection with the numbers listed in Table III. The intensities of the observed γ rays populating a level account, even for the lowest levels, for at most 30% of the depopulating intensity. As a consequence, in several cases we observe γ rays from transitions between two levels in coincidence with γ rays depopulating the lower level but not, or much weaker, in coincidence with γ rays populating the upper level. This reflects itself in large uncertainties in the γ-ray intensities of weak lines in Table III, although these transitions are clearly established.

For comparison we have also included in Table III the results from the transfer reaction experiments. For all levels the possible spin values deduced from the nonzero transfer amplitudes observed in the ^{197}Au$(\vec{d},t)$ reaction are listed. The nonobservation of certain transfer amplitudes as well as comparisons with theoretical angular distributions are not used as arguments to assign spins. Therefore the resulting spin ranges are in some cases larger than those given in Refs. [7,8]. In all cases where definite spin assignments were possible from the ^{198}Hg$(\vec{d},\alpha)$ transfer the spins derived from the $(\vec{d},t)$ transfer [7,8] are given in square brackets following those from the $(\vec{d},\alpha)$ reaction.

A complete list of all γ rays observed in the $\gamma\gamma$ coincidence measurement is given in Ref. [13].

C. $\gamma\gamma$ angular correlations

The Clover detectors in the YRAST Ball array were located in a plane perpendicular to the beam direction. In such a geometry the in-beam angular correlation of a $\gamma\gamma$ cascade, which has in general a complicated form due to the alignment of the initial level of the cascade, can be expanded in terms of Legendre polynomials which are functions of the angle θ between the detectors recording the two γ rays [16]:

$$W(\theta) = 1 + A_2 Q_2 P_2[\cos(\theta)] + A_4 Q_4 P_4[\cos(\theta)]. \quad (1)$$

The angular correlation coefficients A_k depend, in addition to their dependence on the spins and multipolarities involved,

TABLE IV. Angular correlation coefficients for selected $\gamma\gamma$ cascades in ^{196}Au.

E_1 [keV]	E_2 [keV]	E_3 [keV]	I_1	I_2	I_3	A_2	A_4
625.2	162.6	0.0	(4^-)	$2^-,3^-$	2^-	-0.26 *9*	0.17 *11*
349.2	166.4	0.0	2^-	1^-	2^-	-0.15 *9*	0.06 *10*
571.5	212.8	0.0	(4^-)	4^-	2^-	-0.38 *10*	-0.12 *10*
625.2	234.5	6.6	(4^-)	3^-	1^-	-0.23 *10*	-0.10 *11*
625.2	234.5	0.0	(4^-)	3^-	2^-	0.03 *9*	0.24 *12*
568.7	234.5	0.0		3^-	2^-	-0.19 *9*	0.02 *12*
571.5	234.5	0.0	(4^-)	3^-	2^-	-0.23 *9*	0.08 *11*
668.8	234.5	0.0	(3^-)	3^-	2^-	0.06 *10*	0.36 *14*
720.4	234.5	0.0		3^-	2^-	-0.21 *9*	-0.06 *12*
569.8	323.8	41.9	$1^-,2^-,3^-$	1^-	0^-	-0.17 *9*	0.08 *12*
713.9	467.1	84.7		$3^+,4^+$	5^+	-0.17 *9*	0.08 *12*

on the alignment of the initial state with respect to the beam direction. We assume, as customary in nuclear reactions, a Gaussian distribution of the relative populations of the magnetic nuclear substates with a distribution parameter σ [17]. For the solid-angle correction factors Q_k a rough estimate yields $Q_2=0.96$ and $Q_4=0.84$ for the Clover detectors in the YRAST Ball array.

For the determination of experimental angular correlation coefficients the events of the four Clover detectors were sorted into individual $4k\times 4k$ matrices for the six detector combinations with $\theta=40°$, 45°, 82.5°, 147.5°, 167.5°, and 172.5°. The energy dependence of the coincidence efficiency was assumed to be identical for the four Clover detectors and an internal normalization was performed with the help of the $2_2^+\rightarrow 2_1^+\rightarrow 0^+$ $\gamma\gamma$ cascade in ^{196}Pt, which results in our experiment from the decay of the 6.2*d* ground state of ^{196}Au, with known $A_2=0.071$ and $A_4=0.315$.

Unfortunately, we were faced in the analysis of the $\gamma\gamma$ angular correlations with problems presumably caused by an inappropriate normalization. To illustrate this we list in Table IV the A_k coefficients derived for a few strong $\gamma\gamma$ cascades and discuss the results for the two $\gamma_1\gamma_2$ cascades with the 625→235 keV transition as γ_1. The excitation function and the γ depopulation restrict the spin of the 625 keV level to 3^-, 4^-, or 5^-, and the spins of the 235 keV intermediate state and the final 0 and 7 keV states are believed to be established. The A_k coefficients for the $I^-\rightarrow 3^-\rightarrow 1^-$ cascade, taken at face value, would exclude $I^\pi=3^-$ and 5^- for the 625 keV level: for $I=5$ the A_k are positive, and for $I=3$ A_4 is larger than $+0.1$ for $E2/M1$ mixing ratios of the $3^-\rightarrow 3^-$ transition required to explain A_2. The A_2 coefficient for the $4^-\rightarrow 3^-\rightarrow 1^-$ cascade is shown in Fig. 7 to exemplify the dependence of the A_k coefficients on the $E2/M1$ mixing ratio δ and the spin distribution parameter σ. At $Q\geqslant 0.9$ the A_4 coefficient varies between -0.06 and -0.25 for different values of σ in accordance with the experimental result. However, it is now difficult to understand the large experimental A_4 coefficient for the $4^-\rightarrow 3^-\rightarrow 2^-$ cascade. From the conversion-electron measurements described below we found that the 235 keV $3^-\rightarrow 2^-$ transition has predominant $M1$ multipolarity with less than 30% $E2$ content. The A_4 coefficient of the $4^-\rightarrow 3^-\rightarrow 2^-$ cascade is positive, but for $Q_1\geqslant 0.9$, $Q_2\leqslant 0.3$, and $\sigma\geqslant 1$, it is less than $+0.1$, which is barely consistent with the experimental result. Nevertheless, we believe that the $\gamma\gamma$ angular distributions for the two cascades discussed can only be explained with $I^\pi=4^-$ for the 625 keV level and predominant $E2$ multipolarity for the 391 keV transition from the 625 keV level to the 235 keV level.

An additional indication that we have some unverifiable problems with the normalization comes from the fact that we derive for almost all $\gamma\gamma$ angular correlations negative A_2 coefficients, a not very plausible result. We therefore believe that reliable conclusions on spins can only be obtained for those cases, where for the considered $\gamma\gamma$ cascade only one spin is unknown, at least one transition has pure multipolarity, and the A_k coefficients derived in the present work favor very clearly one spin sequence. Unfortunately, these conditions are only fulfilled for three more cases (see Table IV): (i) the 625→163→0 keV cascade, for which the $\gamma\gamma$ angular correlation is not inconsistent with a $4^-\rightarrow 2^-\rightarrow 2^-$ spin sequence; (ii) the 572→213→0 keV cascade, for which the possible spins of the initial 572 keV level are 3, 4, or 5 and

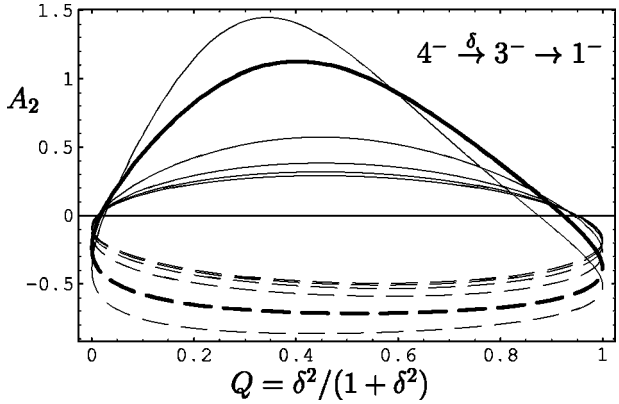

FIG. 7. A_2 coefficient of the $4^-\rightarrow 3^-\rightarrow 1^-$ cascade as a function of the $E2/M1$ mixing ratio δ of the $4^-\rightarrow 3^-$ transition (solid curves: δ positive; dashed curves: δ negative). The various curves are calculated with the distribution parameter $\sigma=0-5$ in steps of 1 (bold curve: $\sigma=1$).

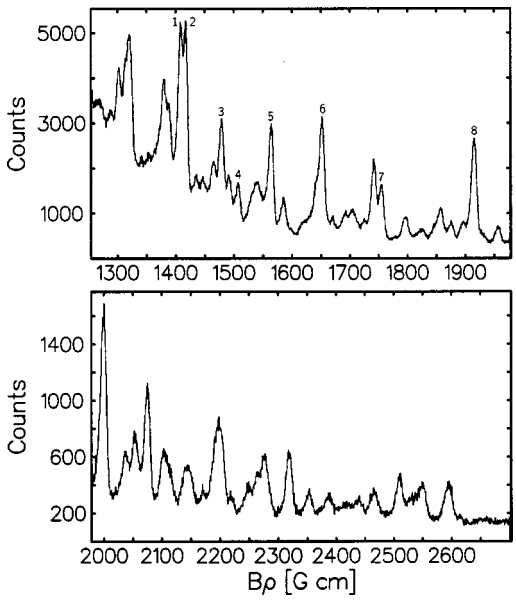

FIG. 8. Singles electron spectrum from $E_{e^-} \approx 125$ to ≈ 445 keV measured following the ^{196}Pt(p,n) reaction at a proton bombarding energy of 9.1 MeV. The spectrum was recorded by stepping the spectrometer current in steps of 0.1 A from 180 to 390 A for a total of 6 h at a beam current of ~ 300 nA. The momentum resolution $\Delta p/p$ was approximately 0.7%. The eight electron peaks, for which $e^-\gamma$ coincidences were measured, are labeled.

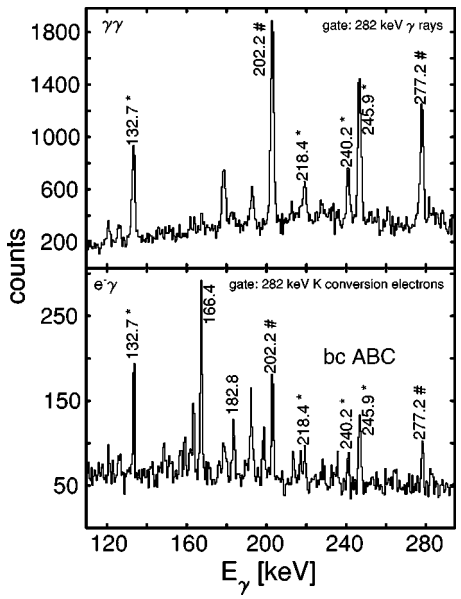

FIG. 9. Comparison of γ-ray spectra measured in coincidence with 202 keV electrons (peak number 6 in Fig. 8) and 282 keV γ rays. The symbols # and * mark the γ rays in coincidence with the 281.6 and 281.9 keV γ rays, respectively, in the decay of ^{196}Au. The unmarked lines in the $e^-\gamma$ spectrum result from coincidences with L- and M-conversion electrons (see, e.g., Table V).

the A_k coefficients are only consistent with $I=4$ and $Q(359\ \text{keV}) \leqslant 0.4$; (iii) the $570 \rightarrow 324 \rightarrow 42$ keV cascade, where $I^\pi = 0^-$ for the 570 keV level is excluded by the $\gamma\gamma$ angular correlation.

To conclude this section, we believe that some as yet unknown spins and parities of levels in ^{196}Au could be determined from $\gamma\gamma$ angular correlations measured in-beam, provided a careful off-beam normalization of the detectors used in the measurement is carried out. Unfortunately, we were not aware of this possibility during the measurements and therefore failed to obtain this normalization.

D. Multipolarities from conversion-electron experiments

Conversion electrons were measured with the iron-free orange spectrometers at the Bonn cyclotron [18]. These spectrometers are used alternatively in three configurations: (i) Singles conversion electrons are recorded with a large spectrometer. Electron spectra are measured with this spectrometer by stepping the current over the region of interest. The pulse height from the electron detector (NE102 plastic scintillator viewed with a photomultiplier), and the time relative to the beam pulse are recorded on magnetic tape and analyzed off-line. (ii) For the measurement of $e^-\gamma$ coincidences four Compton suppressed Ge detectors are placed behind the target opposite to the spectrometer. (iii) A second smaller orange spectrometer is connected to the large one, thus forming a tandem spectrometer used for the measurement of e^-e^- coincidences. The targets used in these measurements were 400 μg/cm^2 thick self-supporting metal foils of enriched ^{196}Pt.

A singles electron spectrum is shown in Fig. 8. The various peaks seen in the spectrum can result in general from a superposition of conversion electrons from different atomic shells. Their composition can be identified by measuring the coincident γ-ray spectra for a comparison with the corresponding $\gamma\gamma$-coincidence spectra. Such measurements have been performed for the electron peaks labeled in Fig. 8.

As an example we compare in Fig. 9 the γ-ray spectrum measured in coincidence with the electrons of the peak number 6 with the corresponding spectrum in coincidence with 282 keV γ rays. This latter γ ray is doubly assigned in the level scheme, as $288.2 \rightarrow 6.6$ keV (281.6 keV) and $323.8 \rightarrow 41.9$ keV (281.9 keV) transition. The corresponding coincident γ rays are marked in Fig. 9 by the symbols # and *, respectively. From the comparison of the two spectra one can conclude that the two 282 keV γ rays have the same multipolarity, and the strength of the peak number 6 in the singles electron spectrum fixes it as $M1$. The results obtained from these $e^-\gamma$ coincidence measurements for the eight peaks labeled in Fig. 8 are summarized in Table V.

Similar $e^-\gamma$ coincidence measurements were already performed during our earlier studies of ^{196}Au in the $(d,2n)$ reaction [11]. From the measurements with the K conversion electrons of 160.9, 162.6, and 166.4 keV transitions we conclude that these transitions have predominant $M1$ multipolarity. In particular, the 162.6 keV γ ray is placed twice in the negative-parity level scheme and similar considerations as those discussed in connection with Fig. 9 establish $M1$ multipolarity for both transitions.

For some strong transitions between levels of equal parity a decision on their multipolarity can be obtained from the $K/\Sigma L$ conversion-electron intensity which is 6.0 for $M1$ and

TABLE V. Assignment of the peaks labeled in Fig. 6.

Peak no.	$B\rho$ [G cm]	E_{e^-} [keV]	Assignment	Multipolarity
1	1409.6	152.0	166.4 L_I	$M1$
2	1418.9	153.9	234.5 K	$M1$
3	1481.2	166.0	246.7 K	$M1$
4	1510.0	171.7	252.2 K	
			252.6 K	
5	1566.3	183.0	263.7 K	$M1$
6	1656.8	201.6	281.6 K	$M1$
			281.9 K	$M1$
			212.8 L_{III}	
			216.0 L_I	
7	1756.6	222.8	303.5 K	$E2$
8	1918.1	258.3	339.0 K	$M1$

$\leqslant 1.5$ for $E2$ multipolarity for γ-ray energies below 250 keV. In the present case this ratio indicates predominant $M1$ multipolarity for the 166.4 and 182.8 keV transitions.

For low-energy transitions the intensities of the conversion electrons from L subshells depend strongly on the transition multipolarities providing a sensitive method for their determination. With our large orange spectrometer we are able to separate the L subshell conversion electrons for transitions with energies below approximately 200 keV. Unfortunately, in the present case the electron spectrum is so complicated that reliable L subshell ratios can only be determined from e^-e^- coincidence measurements (with one exception, see below). Intensity reasons limit this technique to a single, though important, case: the cascade of transitions 141 $\rightarrow$183 keV$\rightarrow$(166 or 125 keV) (see Fig. 12 and the discussion in Sec. III A). All four transitions proceed between levels with negative parity, and thus must have $M1$ or $E2$ multipolarity.

The electron spectrum measured in coincidence with the K conversion electrons of the 183 keV transition is shown in Fig. 10. From the intensity limits of the L_{III} conversion electrons we deduce that all three transitions (125, 141, and 166 keV) have $M1$ multipolarity with less than 20% $E2$ content.

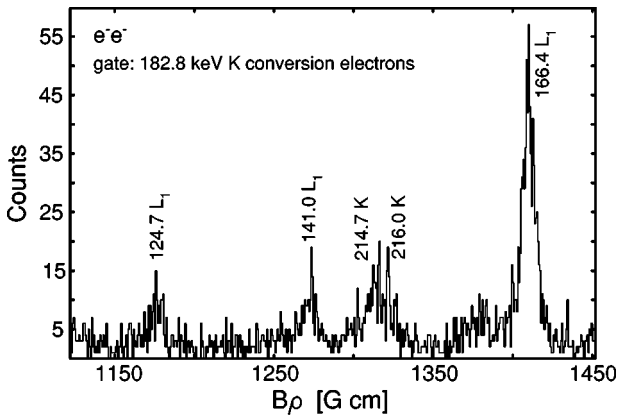

FIG. 10. Electron spectrum in coincidence with K conversion electrons of the 182.8 keV transition in ^{196}Au.

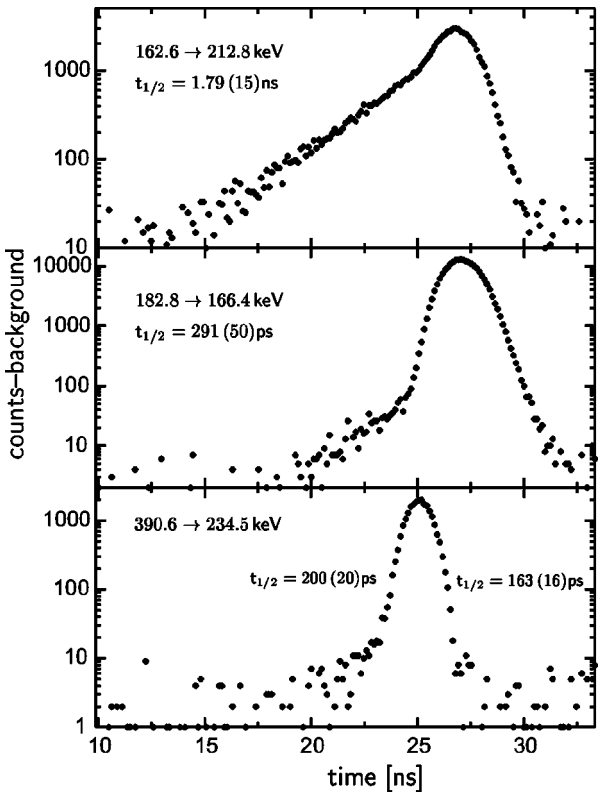

FIG. 11. e^-e^- time spectra for three cascades in ^{196}Au. The start/stop signals for the time-to-amplitude converter were chosen such that the half-life appears to the left for the spectra shown in the upper and lower part, and to the right for the spectrum in the middle part.

Finally, the L subshell intensity ratios of a 213 keV transition could be determined by taking advantage of its delay (see next section), yielding predominant $E2$ multipolarity for this transition.

E. e^-e^- time measurements

From the electron singles measurement described above it is possible to identify conversion electrons with delays larger than approximately 200 ps by setting in the off-line analysis an appropriate window on the time relative to the beam pulse. From such an analysis we found that the 166 and 213 keV transitions from the corresponding levels to the ground state are the only transitions with conversion electrons exhibiting such a delay. We have therefore performed e^-e^- time measurements with cascades via these two levels, as well as one via the ''prompt'' 234.5 keV level. These measurements were performed following the $(d,2n)$ reaction because of its larger cross section.

From the time spectra shown in Fig. 11 we obtain the following results:

166.4 keV level: $t_{1/2}=291\pm 50$ ps,

212.8 keV level: $t_{1/2}=1.79\pm 0.15$ ns,

234.5 keV level: $t_{1/2}\leqslant 200$ ps.

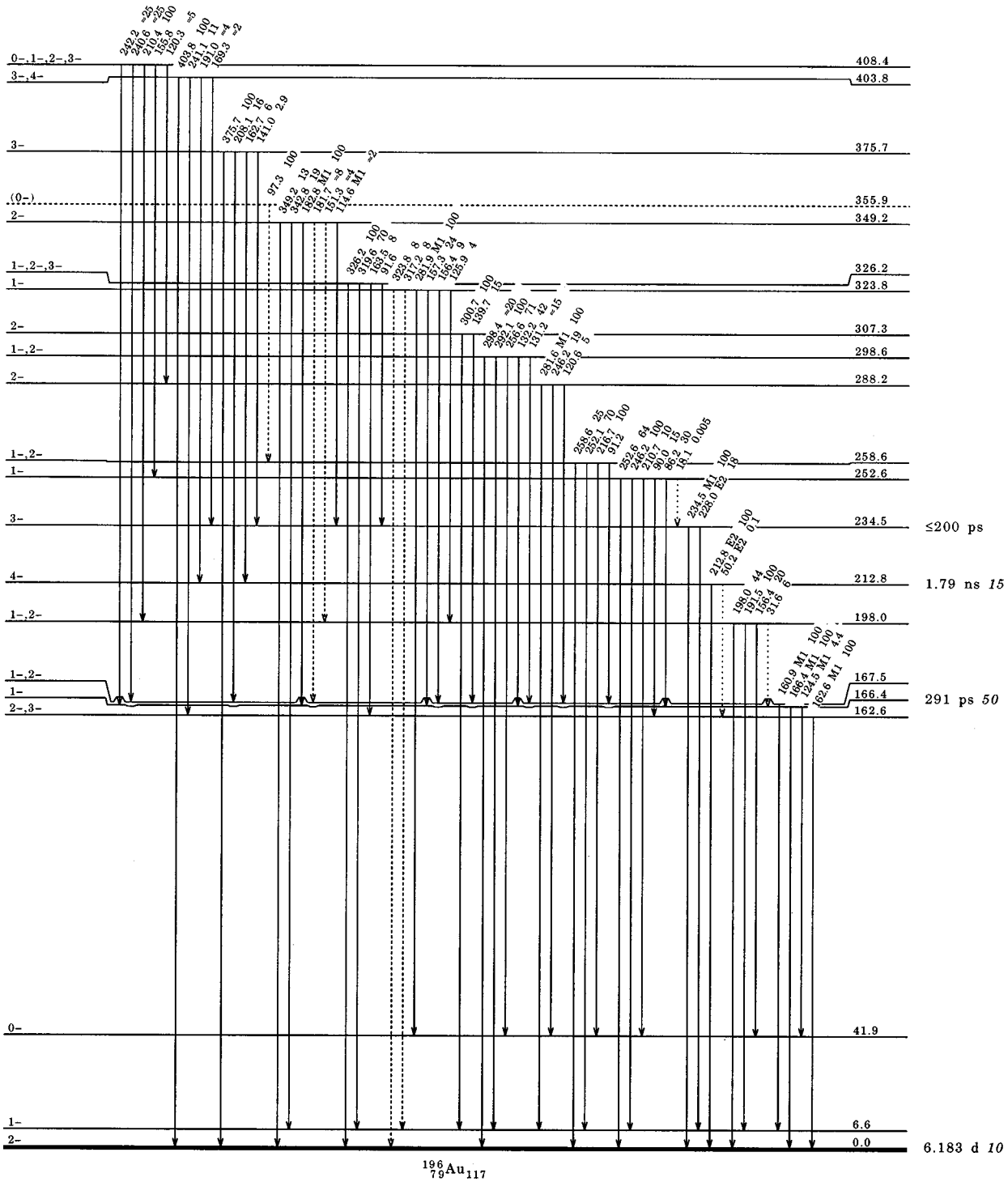

FIG. 12. Level scheme of ^{196}Au showing the negative-parity levels built on the 2^- ground state.

III. DISCUSSION

The level scheme of ^{196}Au determined in the present work consists of two parts: a negative-parity structure built on the 2^- ground state, and a positive-parity structure built on the 8.1 second 5^+ isomer at 84.7 keV [12]. We observe only three weak transitions connecting these two structures, and we will therefore discuss them separately in the following two subsections. The negative-parity levels will then be compared with the predictions of the supersymmetric theory in a final subsection.

A. Level scheme of the negative-parity states in ^{196}Au

The levels observed in the present work, which were known from the transfer reaction experiments to have negative parity ($l=1$ or $l=3$ transfer), are shown in Figs. 12–17 together with those levels, which we observe to populate

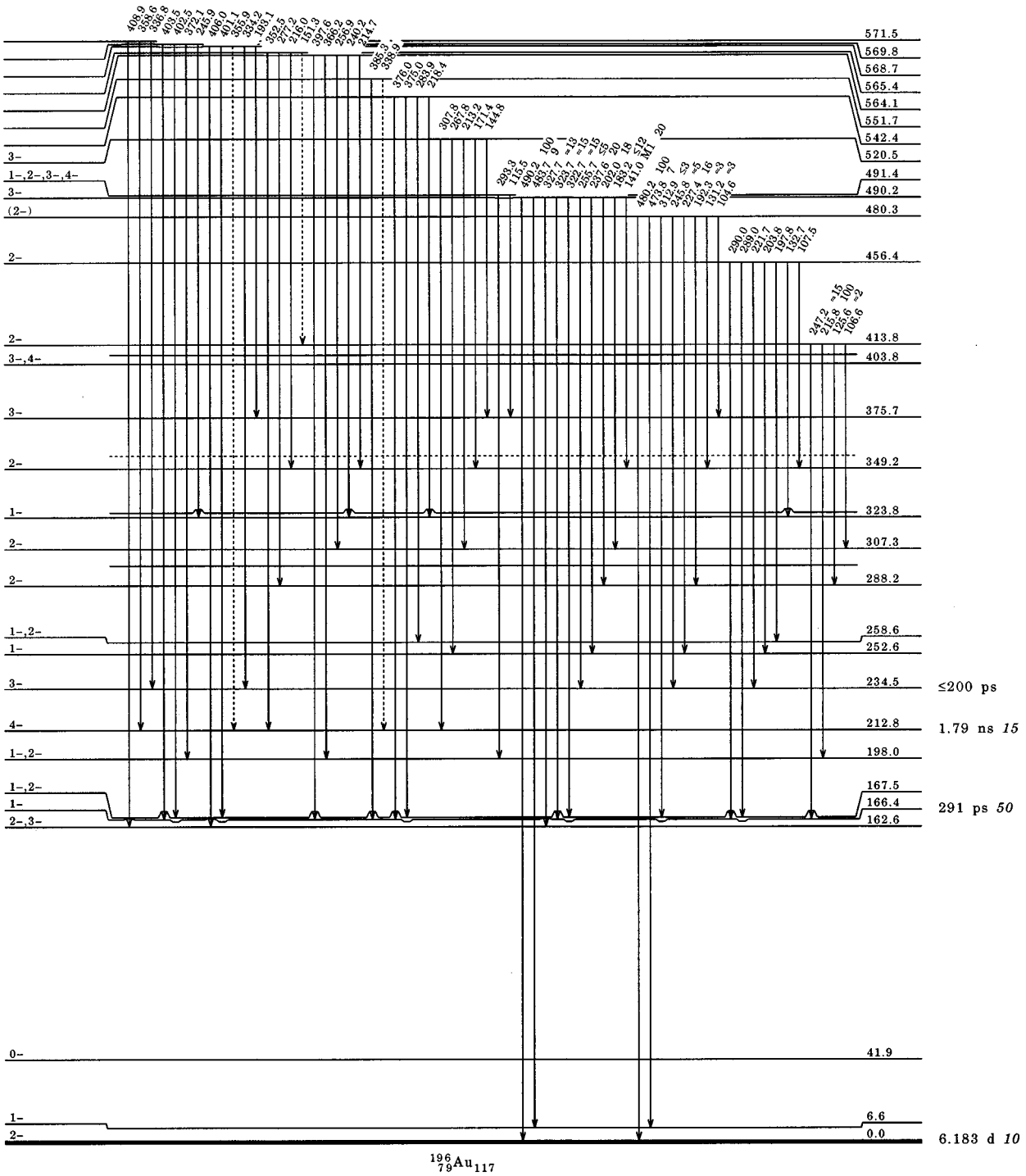

FIG. 13. Level scheme of ^{196}Au (continued).

these negative-parity levels. Despite the complexity of the level scheme most of the assignments given in the figures are safely established by the observation of several transitions populating and depopulating the various levels. A summary of the number of populating and depopulating transitions observed for the levels up to an excitation energy of 820 keV is given in Table VI. For the higher-lying levels we do not observe any populating transitions.

Up to an excitation energy of 800 keV there is an almost perfect correspondence between the levels observed in the present work and those reported in the transfer reaction experiments (Table III and Ref. [8]), with a few notable exceptions: (i) In the transfer reactions a level is observed at 387.5 ± 0.7 keV for which $I^{\pi}=0^{-}$ or 1^{-} is proposed, whereas we observe a 3^{+} level at 388.2 keV (see Secs. II B and III B). The 0^{-} or 1^{-} assignment is based on the angular dependence of the cross section and analyzing power observed in the $(\vec{d},t)$ reaction, but we feel that a 3^{+} assignment is not excluded due to the limited statistical accuracy of these

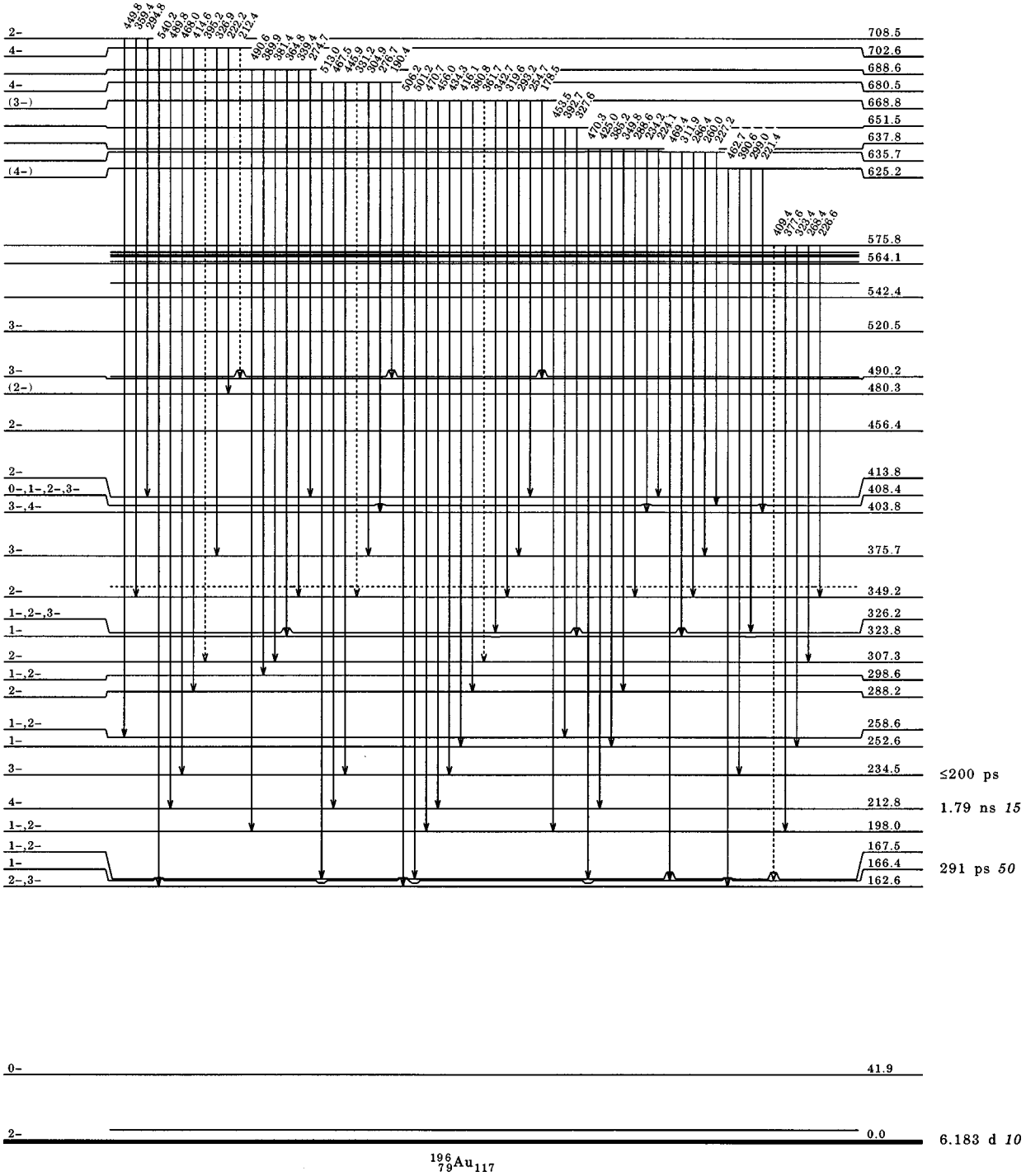

FIG. 14. Level scheme of ^{196}Au (continued).

data for this weakly excited level. (ii) A level is observed in the transfer reactions at 465.5 ± 0.7 keV which is proposed to be a doublet based on an inconsistency of the angular distributions observed for this level in the $(\vec{d},t)$ and $(\vec{d},\alpha)$ reactions. Metz *et al.* assign 1^- [from the $(\vec{d},\alpha)$ reaction] and 3^- [from the $(\vec{d},t)$ reaction] to these two levels. We do not observe a negative-parity level at 466 keV which could be explained if this level is only populated and depopulated by transitions which are not observed in our $\gamma\gamma$ coincidences (see Sec. II B). We observe, however, a level at 467.1 keV with $I^\pi = 3^+$, 4^+, or 5^+ which could perhaps be responsible for the inconsistencies in the angular distributions mentioned above. (iii) We observe a number of close lying levels which could not be resolved in the transfer reactions despite the extremely good energy resolution of 4 keV achieved in the (p,d) reaction (see Table VI). Of particular interest in connection with the supersymmetric scheme are the two addi-

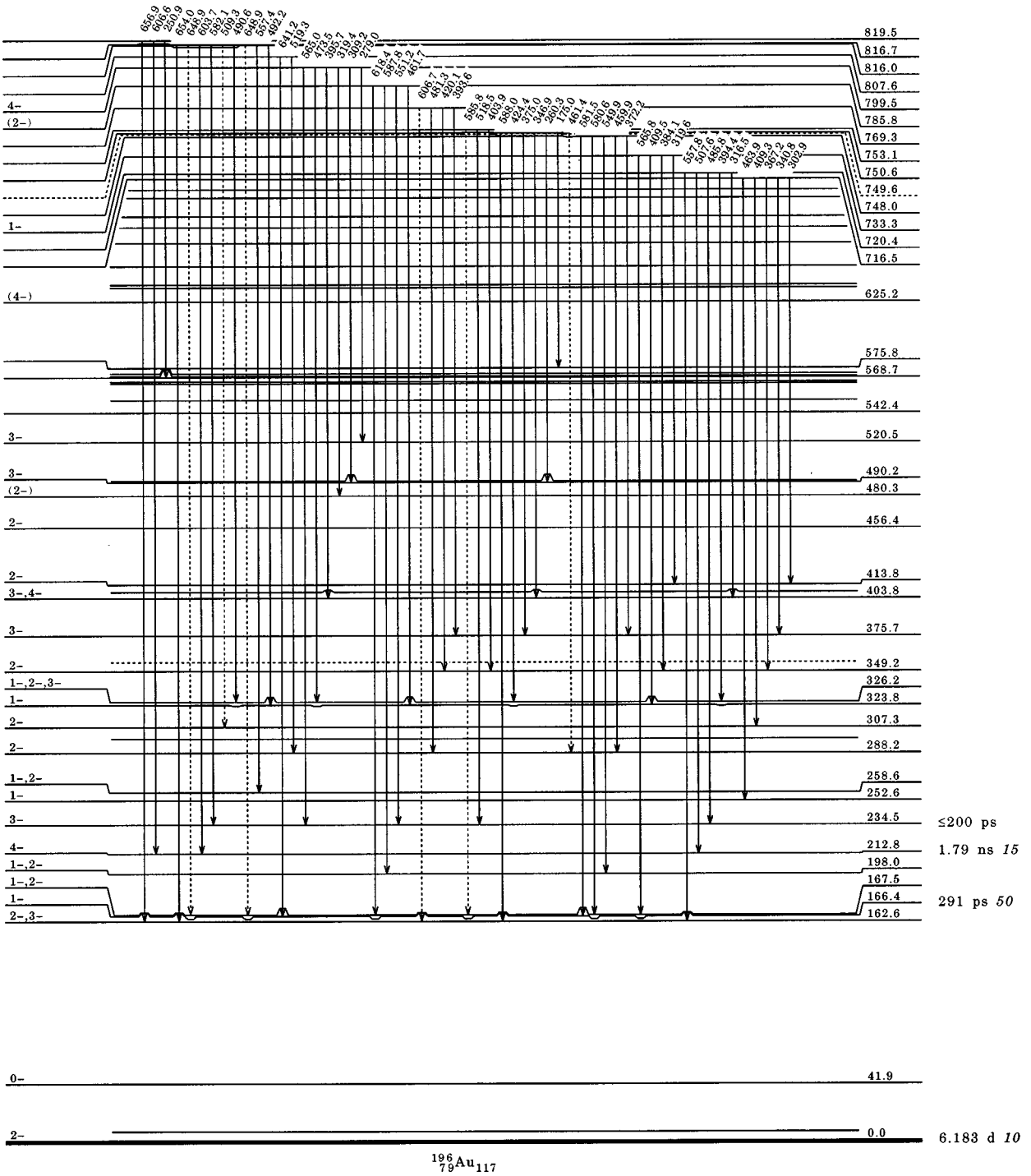

FIG. 15. Level scheme of ^{196}Au (continued).

tional levels below 400 keV, at 166.4 and 326.2 keV, as will be discussed below. (iv) Finally, for some levels, for which negative parity is established from the transfer reactions, our results for the spins are inconsistent with the earlier assignments. These cases will be discussed in detail in the following paragraphs.

A crucial prerequisite for a successful interpretation of the experimental structure of the negative-parity levels within the framework of the quartet supersymmetry is a reliable knowledge of the spins of the excited states. A meaningful restriction of spins from our data on the γ decay of excited levels is only possible if some basic information on spins and parities is already available. Such information is provided by the transfer reaction data of Metz and co-workers [7,8]. These data comprise measurements of the angular dependence of cross sections and analyzing powers in the ^{197}Au$(\vec{d},t)$ and ^{198}Hg$(\vec{d},\alpha)$ reactions with polarized deuterons. A combination of these results provides spin-parity as-

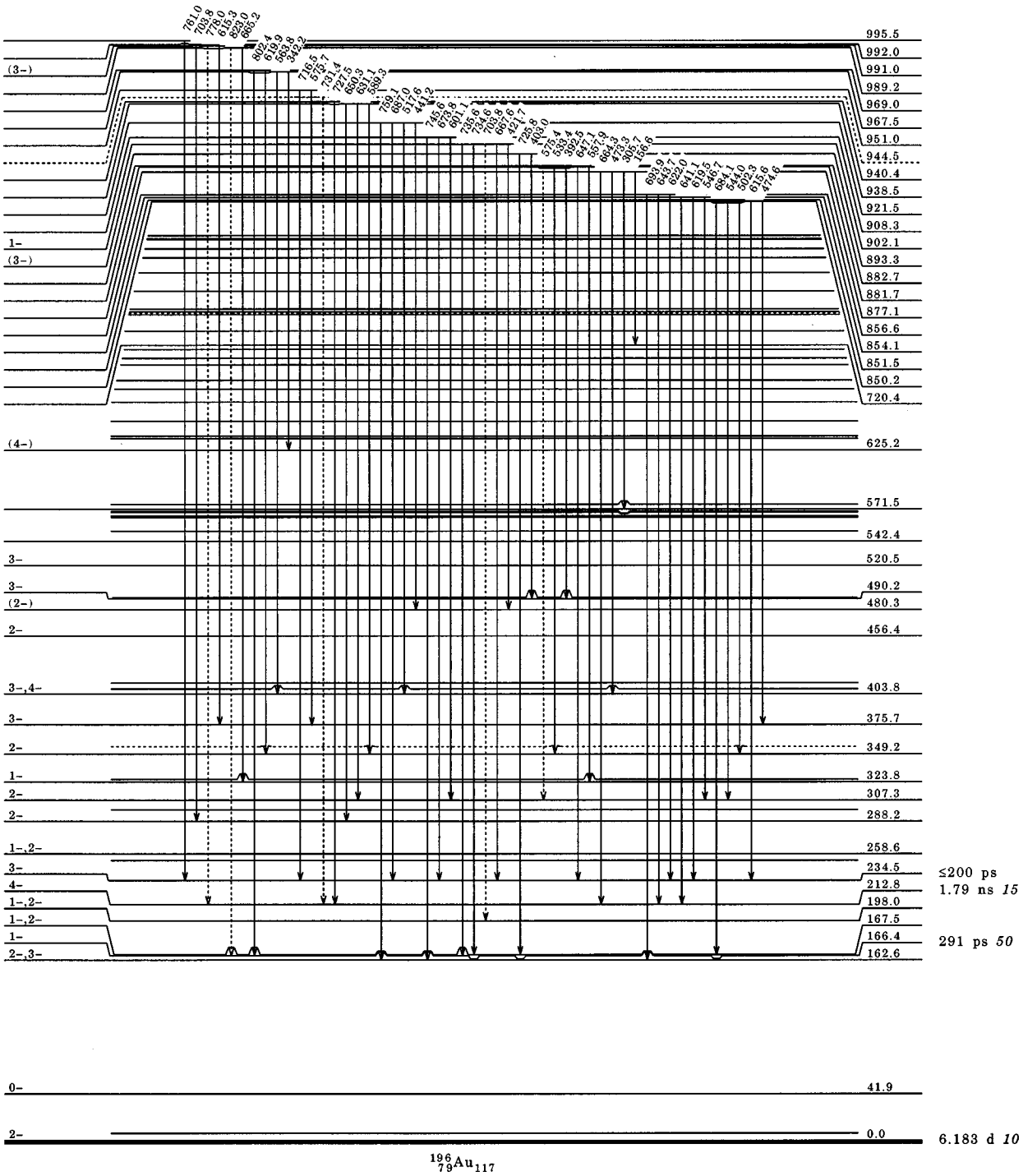

FIG. 16. Level scheme of ^{196}Au (continued).

signments for 28 levels below 1 MeV which are believed to be safely established [19]. The results for the negative-parity levels below 500 keV, which are of interest in the present work, are listed in Table VII. Our data are consistent with these spin-parity assignments, and we therefore accept them as definite. Furthermore, for all levels discussed below the negative parity seems established from the $(\vec{d},t)$ data ($l=1$ or $l=3$ transfer).

Unfortunately, with the above assumptions it is not always possible to derive definite spins if we impose the strict restrictions on the conclusions from the $(\vec{d},t)$ transfer reactions discussed in Sec. II B. We will therefore follow in some cases the procedure already used in our previous work [7,8] and adopt tentative spin assignments by assuming that $I^{\pi}=1^{-}$ and 2^{-} can be excluded for levels, for which both the $p_{1/2}$ and $p_{3/2}$ (l=1) amplitudes are absent in the analysis of the angular distributions observed in the $(\vec{d},t)$ transfer reaction. This assumption seems not unreasonable since in a complex nucleus like ^{196}Au the low-spin levels can be expected to be highly fragmented [8].

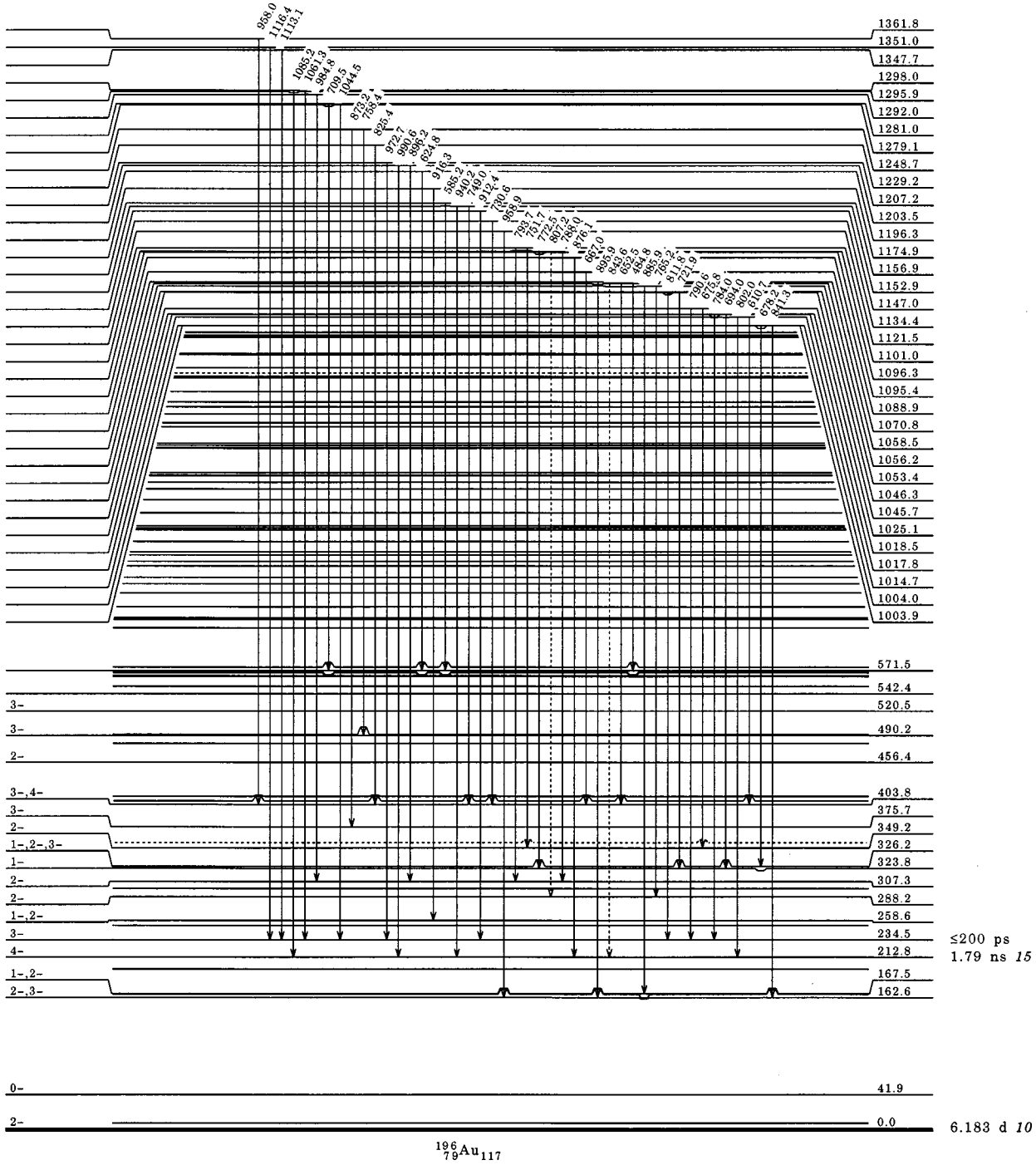

FIG. 17. Level scheme of ^{196}Au (continued).

On the basis of these assumptions we will now discuss the available information on spin parity assignments in detail.

166.4, 198.0, 252.6, 258.6, 288.2, 298.6, and 323.8 keV levels: These levels decay to the 41.9 keV 0^- level which limits their spin parity to 1^- or 2^-. Moreover, for the 166.4 and 323.8 keV levels the transition to the 0^- level has $M1$ multipolarity, yielding $I^\pi=1^-$ for these two levels. Our spin-parity assignments are consistent with those derived from the transfer reaction data except for the 258.6 and 288.2 keV levels. Metz *et al.* observe levels at 257.9 ± 0.6 and 287.4 ± 0.6 keV to which they assign $I^\pi=4^-$ and 3^-, respectively [7,8]. A closer inspection of these data shows that the angular distributions for the 287.4 keV level are incompatible with $I^\pi=1^-$, but not with $I^\pi=2^-$ which we therefore adopt for this level. For the 257.9 keV level, however, the observation of a strong $f_{7/2}$ transfer without any p transfer is difficult to associate with a low spin for this state. One possible reason for this problem, that different levels are observed in the transfer reaction and the (p,n) reaction, seems very implausible.

162.6 keV level: This level decays by an $M1$ transition to the 2^- ground state and is populated from the 403.8 and

TABLE VI. Summary of the excited levels in ^{196}Au up to 800 keV, which are connected with the low-lying levels of negative parity.

$E_{exc.}$ [a] [keV]	Number of transitions Depop.	Pop.	$E_{exc.}$ [a] [keV]	Number of transitions Depop.	Pop.
0.0		15	564.1	5	
6.6		11	565.4[b]	3	
41.9		7	568.7	5	1
162.6	1	20	569.8	4	
166.4	2	18	571.5[b]	3	5
167.5[b]	1	26	575.8[b]	4	1
198.0	4	14	625.2	4	1
212.8	2	23	635.7	5	
234.5	2	34	637.8[b]	7	
252.6	6	7	651.5	3	
258.6	4	7	668.8	13	
288.2	3	15	680.5	7	
298.6	5	1	688.6	6	
307.3	2	18	702.6	8	
323.8	6	11	708.5	3	
326.2[b]	4	8	716.5	4	
349.2	6	23	720.4	5	1
355.9	1		733.3	4	
375.7	4	15	748.0	5	
403.8	4	12	749.6[b]	1	
408.4	5	1	750.6[b]	6	
413.8	4	6	753.1[b]	3	
456.4	7		769.3	4	
480.3	8	3	785.8	3	
490.2	10	7	799.5	6	
491.4[b]	2		807.6	2	
520.5	5	1	816.0	3	
542.4	4		816.7	6	
551.7[b]	1		819.5	3	

[a]The quoted energies have uncertainties of ± 0.1 keV.
[b]Levels not observed in the transfer reaction experiments.

TABLE VII. Spin-parity assignments for levels of ^{196}Au below 500 keV excitation energy deduced from the ^{197}Au$(\vec{d},t)$ and ^{198}Hg$(\vec{d},\alpha)$ reactions.

$E_{exc.}$ [keV] (p,n)	(p,d)	I^π	Source $(\vec{d},t)$	$(\vec{d},\alpha)$
0.0	0.0	2^-	*x*	
41.9 *1*	41.6 *6*	0^-		*x*
212.8 *1*	212.9 *6*	4^-		*x*
307.3 *1*	307.3 *6*	2^-		*x*
375.7 *1*	375.0 *6*	3^-		*x*
413.8 *1*	413.0 *6*	2^-	*x*	*x*
456.4 *1*	455.6 *6*	2^-	*x*	*x*
480.3 *1*	479.8 *6*	2^-	*x*	

702.6 keV levels which are both assigned from the transfer reaction data as 4^- levels. This limits the spin parity of the 162.6 keV level to 2^- or 3^- in agreement with the transfer reaction data.

167.5 keV level: In the transfer reactions this level is not resolved from the closely located 166.4 keV level (the energy of 166.5 ± 0.6 keV derived in the (p,d) reaction indicates that the peak observed in the transfer reactions results predominantly from the 166.4 keV level). The depopulation of the 167.5 keV level by an $M1$ transition to the 6.6 keV 1^- level and the population from the 490.2 keV 3^- level restricts its spin parity to 1^- or 2^-.

234.5 keV level: The $(\vec{d},t)$ data are in accord with $I^\pi = 2^-$, 3^-, or 4^-, but the 2^- assignment seems unlikely because of the absence of the $l=1$ transfer amplitudes. The $M1$ decay to the 2^- ground state excludes the 4^- assignment. $I^\pi = 3^-$ is also most consistent with the observed excitation function for this level (see Fig. 2) and is therefore considered by us as established.

326.2 keV level: This level was not identified in the transfer reaction experiments. The γ-ray depopulation restricts its spin parity to 1^-, 2^-, or 3^-. The observation of a 91.6 keV transition to the 234.5 keV 3^- level and the absence of the γ decay to the 41.9 keV 0^- level is perhaps an indication against a 1^- assignment.

349.2 keV level: This level decays by $M1$ transitions to the 166.4 keV 1^- and 234.5 keV 3^- levels fixing its spin parity to 2^-.

355.9 keV level: From our data this level is only tentatively confirmed on the basis of one depopulating γ ray suggested by the observed $\gamma\gamma$ coincidences. We note here that this level coincides in energy with the first-exited 2^+ level in ^{196}Pt which is strongly populated in our experiment. This makes the detection of a 355 keV γ ray in ^{196}Au more difficult. In the transfer reactions a level is observed at 355.4 ± 0.6 keV. Metz and co-workers [7,8] suggest $I^\pi = 2^-$ or 3^- for this level, but within two standard deviations the experimental data are in agreement with $I^\pi = 0^-$. Such an assignment might also explain our difficulties to observe this level since a 0^- level is expected to be only weakly populated in the (p,n) reaction. We therefore tentatively assume the existence of a level at 355.9 keV with $I^\pi = 0^-$.

403.8 keV level: The $(\vec{d},t)$ data are compatible with $I^\pi = 2^-$, 3^-, and 4^-, but again $I^\pi = 2^-$ seems unlikely because of the absence of the $l=1$ transfer amplitudes. Spin 2 is also inconsistent with the excitation function observed in the (p,n) reaction, whereas $I^\pi = 3^-$ or 4^- is supported by the γ decay of the 403.8 keV level which proceeds to the lower-lying levels with $I^\pi = 2^-$, 3^-, and 4^-.

408.4 keV level: This level is observed in the $(\vec{d},t)$ reaction with a proposed spin parity of 3^-, but 1^- and 2^-, and even 0^-, cannot be excluded from the angular distributions observed in this reaction (we note in this connection that the 408 keV level is the weakest member of an unresolved multiplet, see Fig. 1 of Ref. [7]). The weak population of the 408 keV level in the (p,n) reaction and its γ decay indicate $I \leqslant 2$, although a 3^- assignment cannot strictly be excluded.

490.2 and 491.4 keV levels: In the $(\vec{d},t)$ transfer reaction a level is observed at 490.6 ± 0.6 keV with a proposed $I^\pi=3^-$. We observe a doublet at this energy which makes the interpretation of the angular distributions observed in the transfer reactions questionable, although the γ decay of both members of the doublet is consistent with the 3^- assignment. For the 490.2 keV level $I^\pi=3^-$ is supported by the excitation function, and therefore tentatively assumed in the present work.

520.5 keV level: The spin-parity of this level is restricted by the $(\vec{d},t)$ reaction and its γ decay to 2^- or 3^-. $I^\pi=2^-$ seems unlikely because of the absence of the $l=1$ amplitudes in the transfer and we therefore tentatively assign $I^\pi=3^-$ to this level.

B. Level scheme of the positive-parity states in ^{196}Au

In addition to the negative-parity states built on the 2^- ground state of ^{196}Au discussed in the previous section we observe two almost unconnected level schemes: (i) A structure of levels which is populated in the (p,n) reaction with approximately 25% of the total intensity, and which is based on the 8.1 s 5^+ isomer of ^{196}Au [12]. The low-lying levels of this structure decay by $M1$ and $E2$ transitions to the 5^+ isomer establishing positive parity for these levels. (ii) A second structure based on the positive-parity high-spin states ($I^\pi=6^+$ to 8^+) known from the radioactive decay of the 9.6 h 12^- isomer of ^{196}Au [12]. This structure is only weakly populated in the (p,n) reaction, but strongly in the $(d,2n)$ reaction. We will denote the members of these two level schemes as ''low-spin positive-parity'' and ''high-spin positive-parity'' states although of course the parity is experimentally established only for the lowest levels. These two structures are again only weakly connected which suggests a separate discussion of these two level schemes. Since the present report is concerned primarily with the supersymmetric description of the negative-parity levels we will present these level structures only for completeness without a detailed discussion of their properties.

The level scheme of the low-spin positive-parity states is shown in Figs. 18 and 19. Its placement on top of the 84.7 keV 5^+ isomer is established by the decay of the 388.2 and 713.9 keV levels. The spin-parity assignments given in Fig 18 are based primarily on the population and depopulation of the levels, and the multipolarities of the transitions. In addition to the multipolarities determined from the conversion-electron measurements (see Table V) we deduce $M1$ or $E2$ multipolarity for the 467→388 keV (78.9 keV) transition and $M1$ multipolarity for the 518→348 keV (169.7 keV) transition from γ-ray intensity considerations. For the strong γ rays depopulating the lowest levels additional information could be obtained from the excitation functions which are inconsistent with $I^\pi\leqslant4^+$ for the 348 keV level, $I^\pi\geqslant5^+$ for the 467 keV level and $I^\pi\geqslant6^+$ for the 424 and 518 keV levels.

Essentially all levels shown in Fig. 18 up to approximately 600 keV were also observed in the transfer reaction experiments: (i) Positive-parity levels are reported by Metz [8] at 348.1(6), 502.1(6), 550.8(7), and 645.0(7) keV. The 348.1 keV level is proposed to be a doublet with a positive-parity and a negative-parity member [8] in agreement with our observation of corresponding levels at 348.4 and 349.2 keV. Our placement of a 501.6 keV level in the positive-parity scheme despite the fact that we observe only one depopulating transition to the 323.8 keV 2^- level, is based on the observation of this level in the $(\vec{d},t)$ reaction with angular distributions characteristic for an $i_{13/2}$ transfer, with no indication for contributions from $l=1$ or $l=3$ transfer. We note here that we observe a second positive-parity level at 502.8 keV as shown in Fig. 20. (ii) Metz *et al.* [7,8] observe levels at 387.5(7) keV and 465.5(6) keV which they assign as 0^- level and (1^-+3^-) doublet, respectively. As already discussed above we associate these states with the 388.2 and 467.1 keV levels shown in Fig. 18. (iii) The 423.7 keV level is masked in the transfer reactions by a strongly populated 8^+ level at 420.8 keV (see Fig. 20). (iv) Finally, a strong peak is observed in the transfer reactions at 519.8(6) keV and associated with a level at this energy with $I^\pi=4^-$, whereas we observe two levels at 518.1 and 520.5 keV with positive and negative parity, respectively.

TABLE VIII. $E\lambda$ transitions from the 388.2 keV 3^+ level.

Transition $I_i^\pi\rightarrow I_f^\pi$	E_γ [keV]	$I_{rel.}^\gamma$	$B(E\lambda)/B_W(E\lambda)$
$3^+\rightarrow5^+$	303.6	100	$\geqslant7$
$\rightarrow2^-$	388.2	4.8(5)	$\geqslant3.5\times10^{-7}$
$\rightarrow4^-$	175.5	0.90(9)	$\geqslant7.2\times10^{-7}$

The level scheme of the high-spin positive-parity states is shown in Fig. 20. The lowest levels up to the 421 keV level were known from the decay of the 12^- isomer [12], and Metz reports positive-parity levels at 369.7(6), 399.2(6), 420.1(6), 586.7(6), and 596.9(7) keV [8]. The levels at 645.5, 848.1, and 931.7 keV are also observed in the level scheme of the low-spin positive-parity states (see Fig. 18). All three levels decay to the 348.4 and 370.1 keV levels supporting the spins proposed for these levels.

The most striking feature of the two positive-parity level schemes is the almost complete absence of transitions to the negative-parity states and between these structures. The $E1$ transitions from the positive-parity to the negative-parity levels are strongly hindered as indicated by the decay of the 388.2 keV 3^+ level summarized in Table VIII.

The $B(E2,3^+\rightarrow5^+)\geqslant7$ W.u. [derived from $t_{1/2}(388.2\text{ keV})\leqslant400$ ps, see Sec. II E] is comparable with $B(E2,7^+\rightarrow5^+)=34(4)$ W.u. [12], and thus the $E1$ transitions have hindrance factors of $\sim10^6$. Similar hindrance factors have been found for corresponding transitions in the neighboring nucleus ^{198}Au [20].

A qualitative explanation for the development of different approximately unconnected level structures is suggested by the calculations reported for ^{198}Au [20,21]. Mayerhofer *et al.* [21] performed IBFM calculations with fermions occupying the proton $d_{3/2}$, $s_{1/2}$, $h_{11/2}$ and neutron $p_{1/2}$, $f_{5/2}$, $p_{3/2}$, $i_{13/2}$ orbitals. The low-lying levels have wave functions consisting predominantly of the quasiparticle configurations

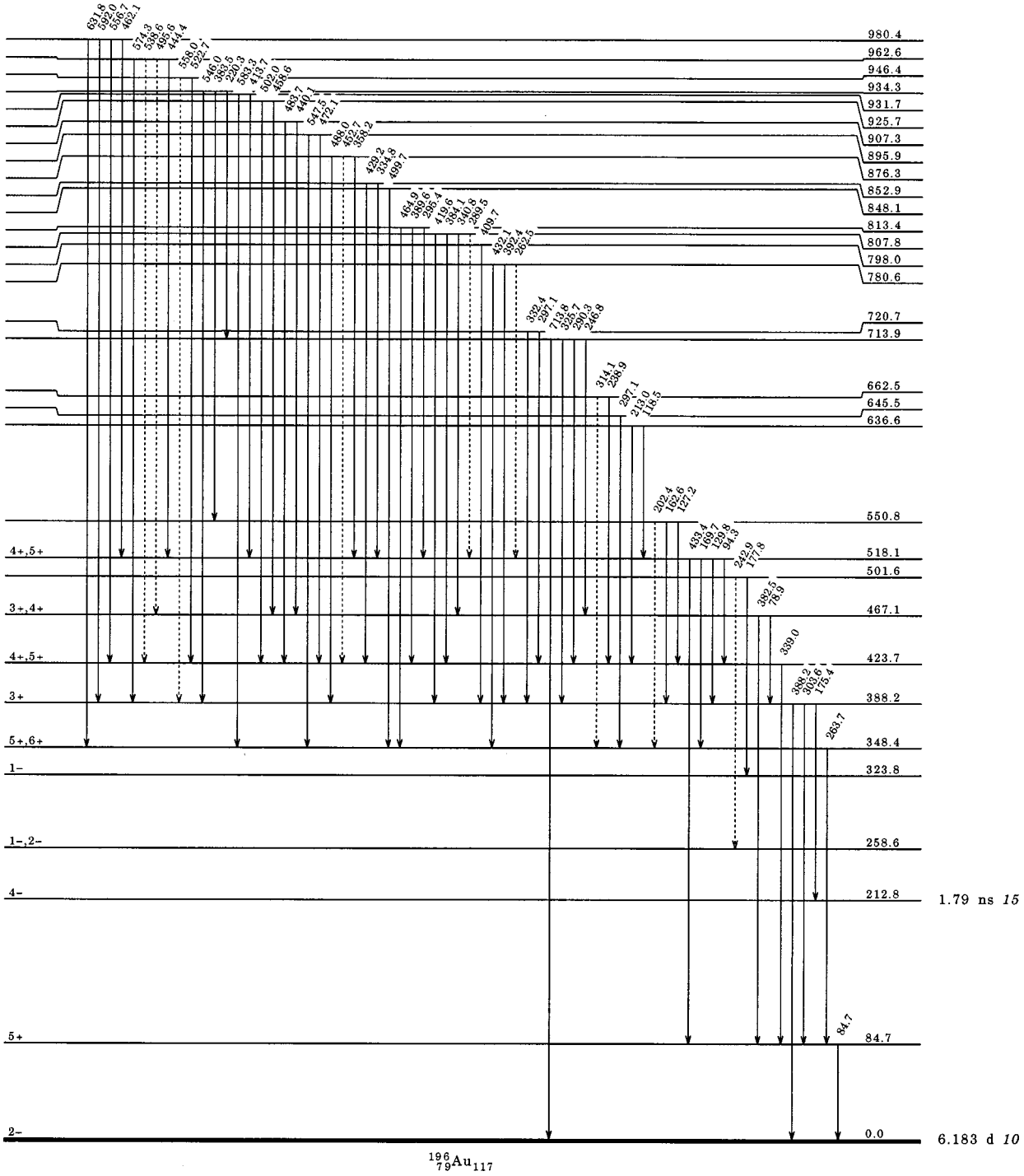

FIG. 18. Level scheme of ^{196}Au showing the low-spin positive-parity levels built on the 5^+ isomer.

$\pi d_{3/2}\nu(p_{1/2},f_{5/2},p_{3/2})$ for negative parity, and $\pi h_{11/2}\nu f_{5/2}$ or $\pi d_{3/2}\nu i_{13/2}$ for positive parity, coupled to few quadrupole phonons. In this approximation all $E1$ transitions are forbidden. Furthermore, one can perhaps expect that the transitions between the positive-parity levels with different $2qp$ configurations are highly hindered compared to those between levels with the same $2qp$ configuration, leading to a natural division of the low-lying positive-parity levels into two only weakly connected structures.

C. Comparison of the negative-parity states with the supersymmetric prediction

As already mentioned in the introduction strong evidence was recently found for the existence of supersymmetry in an investigation of ^{196}Au using the ^{197}Au$(\vec{d},t)$, ^{197}Au(p,d), and ^{198}Hg$(\vec{d},\alpha)$ transfer reactions [7]. In this study some spins of excited states were still uncertain and therefore the comparison of experimental and calculated spectroscopic factors was used as an aid for the assignment of the observed

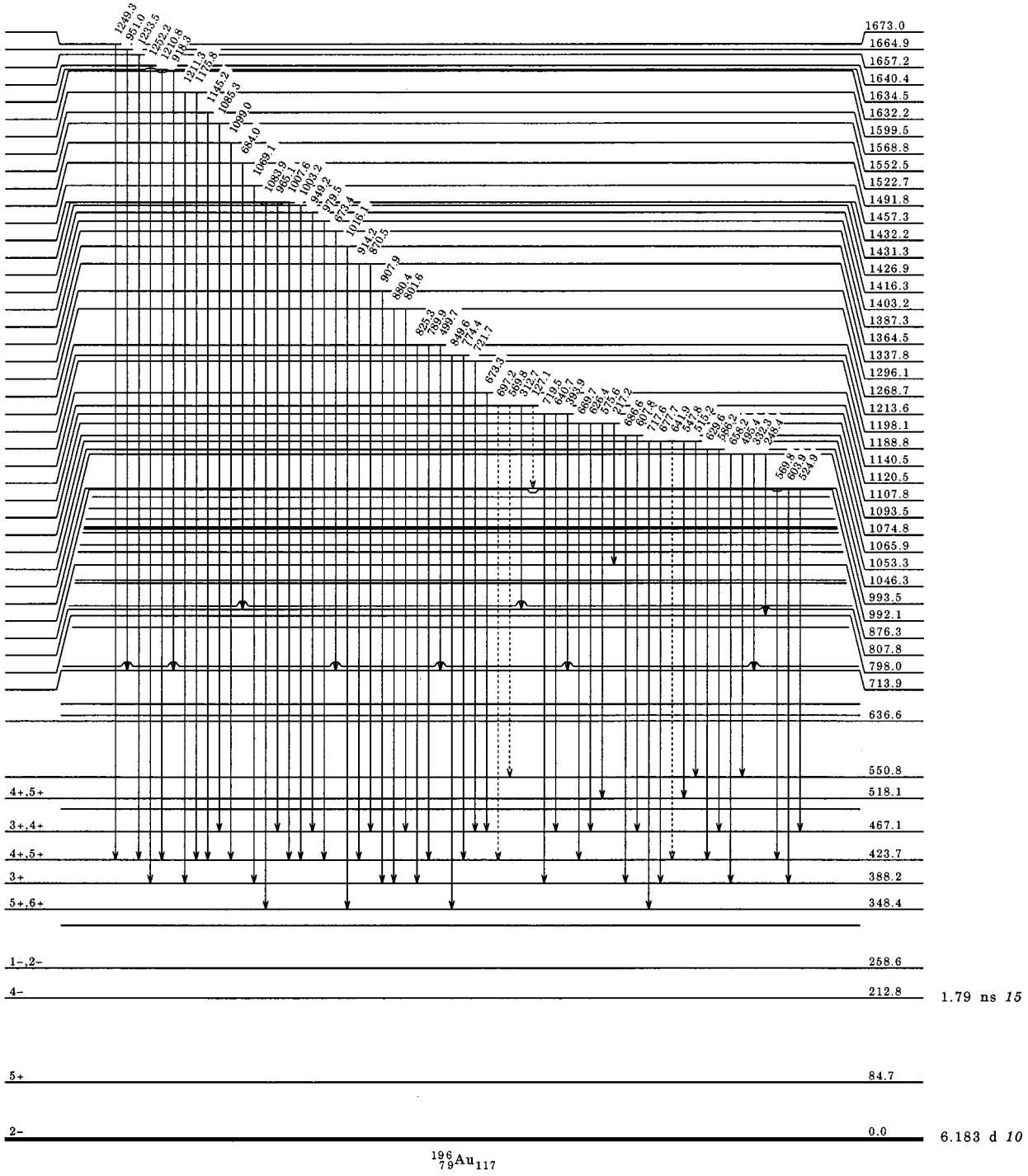

FIG. 19. Level scheme of ^{196}Au (continued).

states to theoretical ones [8]. In this section we will reconsider the supersymmetric description of the negative-parity states of ^{196}Au making use of the new information from the in-beam γ-ray spectroscopy. After a recapitulation of the previous work we will discuss the assignments of the levels in ^{196}Au in detail.

Using the extended $U_\nu(6/12)\otimes U_\pi(6/4)$ supersymmetry, excited states in four neighboring nuclei forming a ''supersymmetric quartet'' can be described by the six-parameter eigenvalue expression [3]:

$$E = A[N_1(N_1+5)+N_2(N_2+3)] + B[\Sigma_1(\Sigma_1+4) + \Sigma_2(\Sigma_2+2)] + B'[\sigma_1(\sigma_1+4)+\sigma_2(\sigma_2+2)+\sigma_3^2] + C[\tau_1(\tau_1+3)+\tau_2(\tau_2+1)] + DL(L+1)+EI(I+1), \quad (2)$$

where A, B, B', C, D, and E are free parameters and $[N_1,N_2],\langle\Sigma_1,\Sigma_2\rangle,\langle\sigma_1,\sigma_2,\sigma_3\rangle,(\tau_1,\tau_2),L,I$ are the quantum numbers correlated to the irreducible representations of

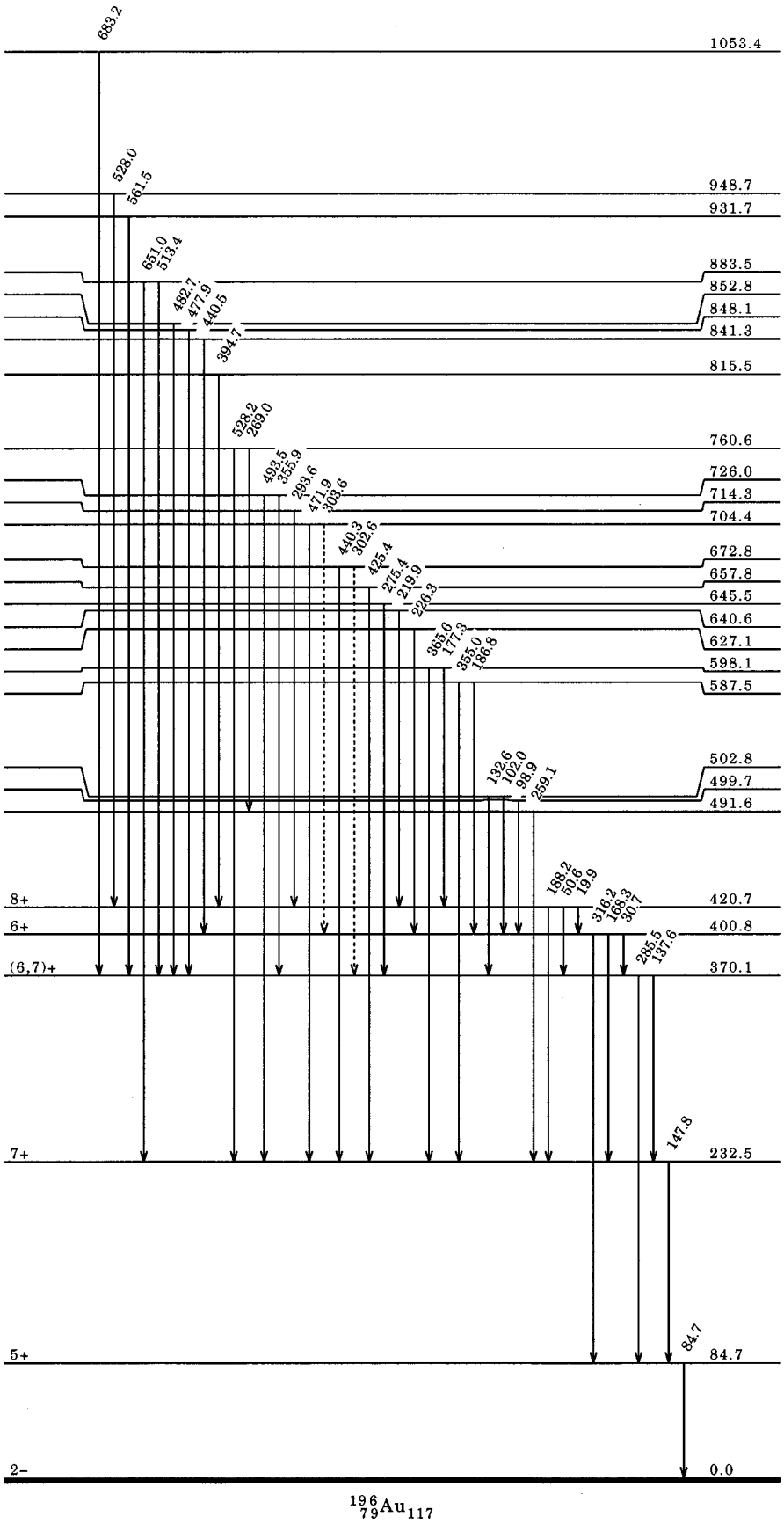

FIG. 20. Level scheme of ^{196}Au showing the high-spin positive-parity levels built on the 5^+ isomer.

$U(6)$, $\overline{O}(6)$, $O(6)$, $O(5)$, $O(3)$, and Spin(3), respectively. The eigenvalue expression can be obtained with the help of the reduction rules given in Refs. [22–24] starting from the dynamical symmetry $U_\nu(6/12)\otimes U_\pi(6/4)$. Using the simple analytic expression of Eq. (2) a quasicomplete description of all observed low-lying excited states in the four nuclei ^{194}Pt, ^{195}Pt, ^{195}Au, and ^{196}Au, forming the supermultiplet, was obtained with a single set of the six parameters [7].

Further evidence for the correctness of the supersymmetric description was provided by the comparison of the experimental and theoretical transfer amplitudes for the states up to 500 keV in ^{196}Au, using a semimicroscopic transfer operator. However, although this comparison provided an excellent additional test of the supersymmetric scheme, some uncertainties remained in the determination of the spins of the excited states. For example, when comparing the experimental spectroscopic strengths for 1^- and 2^- states given by Metz *et al.* (Fig. 3 of Ref. [7]) one notices that both spins often give a similar pattern. The in-beam data reported in the present work provide new and complementary information on the spins which we discuss in the following in detail.

The supersymmetry assignments proposed in the present work for the levels in ^{196}Au up to an excitation energy of $\sim$500 keV are compared with those reported previously by Metz *et al.* [7] in Table IX. For the lowest nine states both assignments agree. We find one new level at 167.5 keV with a proposed $I^\pi=1^-$ which could not be identified in the transfer experiments due to its proximity to the 166.4 keV level. Provided that the 1^- assignment of the 167.5 keV level is correct, this level is remarkable in several respects.

TABLE IX. Supersymmetry assignments for the low-lying levels in ^{196}Au.

Present work		$U_\nu(6/12)\otimes U_\pi(6/4)$ supersymmetry			Theory [a]		Ref. [7] [b]
E [keV]	I^π	$[N_1,N_2]\langle\Sigma_1,\Sigma_2\rangle\langle\sigma_1,\sigma_2,\sigma_3\rangle$	$(\tau_1,\tau_2)L$	I^π	E [keV]		E [keV]
0.0	2^-	[6,0]⟨6,0⟩⟨13/2,1/2,1/2⟩	(1/2,1/2)3/2	2^-	18.0	17.6	0.0*
6.6	1^-	[6,0]⟨6,0⟩⟨13/2,1/2,1/2⟩	(1/2,1/2)3/2	1^-	0.0	0.0	6.0*
41.9	0^-	[5,1]⟨5,1⟩⟨11/2,3/2,1/2⟩	(3/2,1/2)1/2	0^-	120.8	140.6	42.1*
162.6	2^-, 3^-	[5,1]⟨5,1⟩⟨11/2,1/2,1/2⟩	(1/2,1/2)3/2	2^-	145.9	169.2	162.4*
166.4	1^-	[5,1]⟨5,1⟩⟨11/2,1/2,1/2⟩	(1/2,1/2)3/2	1^-	127.8	149.4	166.5*
167.5	1^-, 2^-	[5,1]⟨5,1⟩⟨11/2,3/2,1/2⟩	(3/2,1/2)1/2	1^-	129.9	151.6	
198.0	1^-, 2^-	[5,1]⟨5,1⟩⟨11/2,3/2,1/2⟩	(3/2,1/2)5/2	2^-	218.0	222.2	197.8*
212.8	4^-	[5,1]⟨5,1⟩⟨11/2,3/2,1/2⟩	(3/2,1/2)7/2	4^-	342.3	332.1	212.9*
234.5	3^-	[5,1]⟨5,1⟩⟨11/2,3/2,1/2⟩	(3/2,1/2)5/2	3^-	245.0	248.6	233.5*
252.6	1^-	[6,0]⟨6,0⟩⟨13/2,1/2,1/2⟩	(3/2,1/2)1/2	1^-	217.3	229.8	252.5*
258.6	1^-, 2^-	[5,1]⟨5,1⟩⟨11/2,1/2,1/2⟩	(3/2,1/2)1/2	1^-	345.4	381.4	348.1
288.2	2^-	[6,0]⟨6,0⟩⟨13/2,1/2,1/2⟩	(3/2,1/2)5/2	2^-	305.6	302.6	307.3
298.5	1^-, 2^-	[5,1]⟨5,1⟩⟨11/2,3/2,1/2⟩	(3/2,3/2)3/2	1^-	302.4	320.4	298.3*
307.3	2^-	[5,1]⟨5,1⟩⟨11/2,3/2,1/2⟩	(3/2,3/2)3/2	2^-	320.4	338.0	323.4*
323.8	1^-	[5,1]⟨5,1⟩⟨11/2,3/2,1/2⟩	(5/2,1/2)3/2	1^-	497.4	520.8	465.5
326.2	1^-, 2^-, 3^-	[6,0]⟨6,0⟩⟨13/2,1/2,1/2⟩	(3/2,1/2)5/2	3^-	332.6	329.4	355.4
349.2	2^-	[5,1]⟨5,1⟩⟨11/2,3/2,1/2⟩	(3/2,3/2)5/2	2^-	364.2	372.5	413.0
355.9	(0^-)[c]	[6,0]⟨6,0⟩⟨13/2,1/2,1/2⟩	(3/2,1/2)1/2	0^-	208.4	221.0	
		[5,1]⟨5,1⟩⟨11/2,1/2,1/2⟩	(3/2,1/2)1/2	0^-	335.9	372.6	387.5
375.7	3^-	[5,1]⟨5,1⟩⟨11/2,3/2,1/2⟩	(3/2,1/2)7/2	3^-	306.3	296.9	287.4
403.8	3^-, 4^-	[6,0]⟨6,0⟩⟨13/2,1/2,1/2⟩	(3/2,1/2)7/2	4^-	430.0	412.5	257.9
408.4	0^- to 3^-	[6,0]⟨6,0⟩⟨13/2,1/2,1/2⟩	(3/2,1/2)7/2	3^-	393.9	377.3	375.0
413.8	2^-	[5,1]⟨5,1⟩⟨11/2,1/2,1/2⟩	(3/2,1/2)5/2	2^-	433.5	454.2	455.6
456.4	2^-	[5,1]⟨5,1⟩⟨11/2,3/2,1/2⟩	(5/2,1/2)3/2	2^-	515.8	538.4	479.8
480.3	2^-	[5,1]⟨5,1⟩⟨11/2,3/2,1/2⟩	(5/2,1/2)5/2	2^-	559.2	572.9	564.1
490.2	3^-	[5,1]⟨5,1⟩⟨11/2,1/2,1/2⟩	(3/2,1/2)5/2	3^-	460.5	480.6	465.5
		[5,1]⟨5,1⟩⟨11/2,3/2,1/2⟩	(3/2,3/2)5/2	3^-	390.6	398.9	407.4
491.4	1^- to 4^-	[5,1]⟨5,1⟩⟨11/2,3/2,1/2⟩	(3/2,3/2)9/2	4^-	567.4	544.5	402.5
		[5,1]⟨5,1⟩⟨11/2,3/2,1/2⟩	(3/2,3/2)5/2	3^-	390.6	398.9	407.4
520.5	2^-, 3^-	[5,1]⟨5,1⟩⟨11/2,1/2,1/2⟩	(3/2,1/2)7/2	3^-	521.8	528.9	490.6

[a]First column (second column): energies calculated with the new (old) parameters of the eigenvalue expression [second column (third column) of Table X]. The listed values are the energy differences relative to the lowest level.

[b]Levels obtained in the transfer reaction experiments to which Metz *et al.* [7] assign the listed supersymmetry configurations. The levels for which these assignments agree with ours are marked with an asterisk.

[c]This level is not safely established in our work and the suggested 0^- assignment is very tentative (see Sec. III A).

First, it is observed close to the predicted energy of 152 keV for the missing $(3/2,1/2)1/2,\ 1^-$ member of the $\langle 11/2,3/2,1/2\rangle$ structure (for simplicity we denote these structures with $N_1=5$ by $\langle\sigma_1,\sigma_2,\sigma_3\rangle$ and the $N_1=6$ structure by $[6]\langle 6\rangle$). Second, it is only separated by 1.2 keV from the 1^- state at 166.4 keV indicating that the two 1^- levels are only weakly coupled ($H_{coupl.}\leqslant 0.6$ keV), which is consistent with the presence of a dynamical symmetry. Third, the summed strength of the two states explains the measured strength for the 166.5 keV level observed in the $(\vec{d},t)$ reaction.

Two additional remarks of caution are required in connection with the states observed up to 250 keV. First, the spins of the levels at 162.6 and 167.5 keV are not yet clearly determined by experiment. For example, these two levels could be the lowest excited 3^- and 2^- levels, respectively, which would then influence the assignments of all higher-lying levels. An unambiguous determination of these spins would therefore be very important. Second, two low-lying 0^- levels are predicted by the theory, at 141 and 221 keV, whereas only one such level is identified until now in this energy region, the 42 keV level. We associate this latter level with the lower one of the predicted two low-lying 0^- levels. If a second one exists around 220 keV it could have been masked in the spectra measured in the transfer reactions by one of the strongly populated levels in this energy region. In the (p,n) reaction 0^- levels are expected to be only weakly excited, and one at $\sim$220 keV could easily have escaped detection in the measurement of $\gamma\gamma$ coincidences.

For the states above 250 keV the present work revealed changes for some spins, causing the necessity for many rearrangements in the 250−500 keV region. In the following we will discuss the new assignments state by state with special emphasis on the requirement, that they are consistent with the transfer results of Metz *et al.* [7].

259 keV level: In the previous work $I^\pi=4^-$ was assigned to this state because it is only populated via $f_{5/2}$ transfer in the $(\vec{d},t)$ reaction, whereas the in-beam data yield $I^\pi=1^-$ or 2^-. In order to reassign quantum numbers for this state we take account of the weak transfer amplitudes and assign it tentatively to be the 1^- member of the $(3/2,1/2)1/2$ doublet belonging to the $\langle 11/2,1/2,1/2\rangle$ structure. This configuration was previously assigned to the 349 keV state which is now found to have spin 2.

288 keV level: In the $(\vec{d},t)$ reaction $I^\pi=2^-$ or 3^- was assigned to this state, based on its population via $p_{3/2}$, $f_{5/2}$, and $f_{7/2}$ transfer, and it was proposed to be the lowest 3^- state of the $\langle 11/2,3/2,1/2\rangle$ structure. The in-beam data exclude, however, a spin parity of 3^-. We therefore reassign this level to the $(3/2,1/2)5/2,2^-$ member of the $\langle 13/2,1/2,1/2\rangle$ structure, which is populated in the $(\vec{d},t)$ reaction with a very similar pattern. Since this configuration was previously assigned to the experimental 307 keV state we will have to reassign this state below.

307, 324, and 349 keV levels: The 324 keV level has $I^\pi=1^-$ in contrast to the 2^- assignment proposed by Metz *et al.* We therefore assign the 307 keV 2^- and 324 keV 1^- levels to the $(3/2,3/2)3/2,2^-$ and $(5/2,1/2)3/2,1^-$ configurations of the $\langle 11/2,3/2,1/2\rangle$ structure, respectively. These changes improve the description of the transfer amplitudes. The 349 keV state with its weak transfer strengths is now assigned to the higher lying $(3/2,3/2)5/2,2^-$ configuration which was earlier assigned to the 414 keV level.

326 keV level: This new level is assigned to be the $(3/2,1/2)7/2,3^-$ member of the $[6]\langle 6\rangle$ structure. This assignment is still uncertain since the 326 keV level is part of an unresolved doublet in the transfer experiments and therefore no transfer amplitudes are known for this level.

356 and 388 keV levels: We assign very tentatively a 356 level with spin and parity of $I^\pi=0^-$, while we do not observe a $I^\pi=0^-$ state at 388 keV, but instead a $I^\pi=3^+$ state. We associate the 356 keV level with the 0^- member of the $[6]\langle 6\rangle$ structure. An alternatve assignment, indicated in Table IX, would be the $(3/2,1/2)1/2,0^-$ member of the $\langle 11/2,1/2,1/2\rangle$ structure. However, with this latter assignment it is difficult to account for the observed large $p_{3/2}$ transfer and we therefore prefer the first assignment given in Table IX.

376 keV level: On the basis of the transfer amplitudes this level can clearly be assigned to the $(3/2,1/2)7/2,3^-$ member of the $\langle 11/2,3/2,1/2\rangle$ structure.

404 keV level: In our previous work the 258 keV level was considered to be the second 4^- state predicted at 412.5 keV. With our new assignments it is obvious that the 404 keV level is the candidate for this state. The good agreement for the spectroscopic strengths confirms this assignment. This choice leads to a substantial improvement in the description of the energy and spectroscopic strength of the 4^- member of the $[6]\langle 6\rangle$ structure.

408 keV level: Based on the distribution of the spectroscopic strengths we propose that this level corresponds to the 3^- member of the $[6]\langle 6\rangle$ structure with the quantum numbers $(3/2,1/2)5/2$. Because of the not well determined spin of the 408 keV level this assignment can only be considered as tentative.

414, 456, and 480 keV level: These three 2^- levels are reassigned to the energetically next theoretical states (see Table IX). This improves the description of the transfer strengths for the 413 keV level, while those of the 456 and 480 keV levels are small, both in experiment and theory. For the energies a degradation of the agreement is observed.

490 and 491 keV level: The 490 keV level is assigned as the $(3/2,1/2)5/2,3^-$ member of the $\langle 11/2,1/2,1/2\rangle$ structure on the basis of the $p_{3/2}$, $f_{5/2}$, and $h_{9/2}$ transfer strengths derived for a level observed in the transfer reactions at 490.6 ± 0.6 keV. However, as the latter level is presumably a doublet this assignment is still uncertain, and we therefore list an alternative possibility in Table IX. The 491 keV level could correspond to the 3^- or 4^- member of the $\langle 11/2,3/2,1/2\rangle(3/2,3/2)$ states. This assignment should, however, be considered as very tentative because of the uncertain spin of the 491 keV level.

521 keV level: This level is assigned to the $(3/2,1/2)7/2\ 3^-$ member of the $\langle 11/2,1/2,1/2\rangle$ structure, which is strongly supported by the transfer strengths.

A graphical comparison of the experimental negative-parity levels in ^{196}Au, arranged according to the assignments discussed above, with the predictions of the supersymmetric

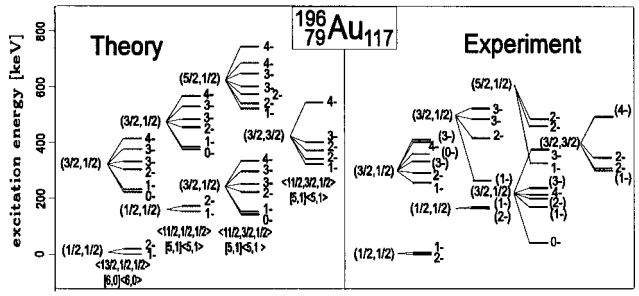

FIG. 21. Comparison of theoretical and experimental levels forming the supersymmetry multiplets in ^{196}Au.

theory [7] is shown in Fig. 21.

We have performed a new fit of Eq. (2) to the supersymmetric levels in the four nuclei forming the supermultiplet using the assignments of the present work. This fit is more restricted than the earlier one [7,8], but nevertheless still deals with 78 levels (eight levels in ^{194}Pt, 32 in ^{195}Pt, 11 in ^{195}Au, and the 27 levels in ^{196}Au assigned above). For ^{195}Au and the two Pt isotopes the assignments given in Ref. [7] are used. A detailed account of the assignments in the Pt isotopes can be found in Ref. [25]. The resulting parameters are compared in Table X with those of Ref. [7] and a parameter set obtained from a fit of Eq. (2) to the supersymmetric levels in ^{194}Pt, ^{195}Pt, and ^{195}Au. The energies calculated with the two parameter sets derived including the levels in ^{196}Au are listed in Table IX to illustrate their dependence on the parameters.

The new parameters exhibit only significant changes, compared to those derived earlier [7], in the parameters B, B', and D. The change in B and B' is related to the fact that the level energies in the platinum nuclei depend only on the sum $B+B'$, and in ^{195}Au only one level is experimentally observed up to now for which the energy depends on B and B' separately (this level is reproduced exactly with the parameters given in the last column of Table X). As a consequence, the sum $B+B'$ is almost unchanged for the different fits, whereas with our present experimental knowledge of levels in the gold isotopes the relative weight of B and B' depends sensitively on the levels in ^{196}Au. The change in B and B' from Ref. [7] to the present work is predominantly caused by the slight decrease of the average excitation energy of the third structure shown in Fig. 21 ($[5,1]\langle 5,1\rangle\langle 11/2,3/2,1/2\rangle$ structure). A dedicated experimental investigation of the structure of ^{195}Au could contribute to a better determination of B and B'.

TABLE X. Parameters of the eigenvalue expression Eq. (4).

Parameter	Results of fits (in keV)		
	this work	Ref. [7]	without ^{196}Au
A	52.5	52.3	51.2
B	8.7	12.4	7.9
B'	−53.9	−58.0	−52.6
C	48.8	50.1	49.0
D	8.8	6.9	6.9
E	4.5	4.4	6.2

The change in D is related to the systematic deviation of the excitation energies of the 4^- states from the predicted ones reported in Ref. [7], which is removed with the new spin assignment of the 259 keV level. The parameters D and E determine the final splitting of the states. They are mainly obtained from the levels in ^{195}Pt and ^{196}Au. We note here that the sum $D+E$ is almost constant for the fits listed in the second and last column of Table X.

In general one can further test the theory using the measured γ-ray branchings and, when available, the measured absolute electromagnetic transition rates. However, in heavy odd-odd nuclei a major problem is encountered for such a comparison. The transitions between excited states have in general dominant $M1$ multipolarity. It is well known that the interacting boson approximation is not very successful in predicting $M1$ transitions in odd-A nuclei (see, for instance, the discussion by Warner in Ref. [26]). When the model fails by several orders of magnitude in these simpler systems, it cannot be expected to describe the more complex odd-odd nuclei. Moreover, due to the high level density almost all excited states decay by at least one $M1$ branch, making also a comparison of the branching ratios questionable.

One exception is the decay of the lowest 4^- state at 213 keV, which decays by an $E2$ transition to the 2^- ground state. For this state the lifetime was measured (see Sec. II E) and one obtains $B(E2;4_1^-\rightarrow 2_1^-)=(4.9\pm 0.5)\times 10^{-2}\ e^2\mathrm{b}^2$. Using the $E2$ transition operator defined by the study of the odd-A nuclei in this mass region ($e_b=e_\pi=-e_\nu=0.151\ e\,\mathrm{b}$) the theory predicts $B(E2;4_1^-\rightarrow 2_1^-)=3.2\times 10^{-2}\ e^2\mathrm{b}^2$. A second $B(E2)$ value can be obtained for the 235 keV 3^- level. From the lifetime estimate and γ-ray branching ratio given in Sec. II one obtains $B(E2;3_1^-\rightarrow 1_1^-)\geqslant 4\times 10^{-2}\ e^2\mathrm{b}^2$. This should be compared to the theoretical value of $B(E2;3_1^-\rightarrow 1_1^-)=5\times 10^{-3}\ e^2\mathrm{b}^2$ which is eight times smaller. One might wonder whether this problem could be solved by a rearrangement of the assignments, because the second theoretical 3^- state has a larger $B(E2;3_2^-\rightarrow 1_1^-)=2.7\times 10^{-2}\ e^2\mathrm{b}^2$. The main problem is that both states have very different signatures in the transfer experiments: dominant and strong $f_{5/2}$ and $p_{3/2}$ transfer strength for the 3_1^- and 3_2^- state, respectively. Exactly this behavior was found for the 235 and 376 keV states. We note here, that the only state with a similar behavior as the 235 keV level is the 162 keV level. However, if the 162 keV level is the 3_1^- state, the 235 keV level does not have the required distribution of transfer strengths to be the 3_2^- state. It should also be mentioned that both transitions discussed above are not very strong. The strongest $E2$ transitions obtained in the calculation have $B(E2)$ values around $0.2\ e^2\mathrm{b}^2$.

IV. CONCLUSION

The present investigation of the nuclear structure of ^{196}Au by in-beam γ-ray spectroscopy is part of an experimental program to test whether ''quartet supersymmetry'' exists in atomic nuclei. For the negative-parity levels, which are of interest in this context, our results for the energies of the levels up to approximately 500 keV are in almost perfect

agreement with those obtained previously in transfer reaction experiments. Some uncertainities remain, however, for the spins, which are of crucial importance for the comparison of the experimental level structure with the predictions of the supersymmetric theory. It is also important to emphasize that we might have failed to identify low-lying excited levels because of the limited sensitivity of the $\gamma\gamma$ coincidence setup used in the present work. This is particularly true for the important $I^{\pi}=0^{-}$ levels, which are expected to be only weakly populated in the compound reaction, whereas the low-lying levels with $I^{\pi}\geqslant 2^{-}$ are strongly populated and are therefore perhaps more completely identified, at least up to excitation energies of approximately 500 keV.

When comparing experiment with theory, excellent agreement is obtained for the states below 250 keV. The spin-parity assignments derived earlier from the transfer reaction experiments are confirmed, and one missing state predicted by the supersymmetric theory could be identified. This is important because at these low energies three different structures appear, and their relative positions largely determine the rest of the level structure of ^{196}Au. The relatively low level density below 250 keV also enables a more clear comparison of the transfer strengths observed in the (d,t) reaction with the theoretical predictions than for the higher-lying levels.

At higher excitation energies the change of the spins of some levels, most notably the 259 keV level, caused the need for many reassignments of quantum numbers to levels above 250 keV. The new assignments are based on more reliable spin values, deduced from the combination of the in-beam work and the transfer experiments, as well as on the observed transfer strengths.

In general the comparison of the experimental energies with those predicted by the supersymmetric theory is quite satisfactory up to 500 keV. Nevertheless, some assignments are still tentative and further experiments are needed for their clarification. The parameters of the supersymmetric eigenvalue expression, obtained from a new fit of this expression to the experimental level energies, show only minor deviations from the ones given in Ref. [7] indicating the importance of the lowest lying levels in defining the supersymmetric level structures. Moreover, the new parameter values are close to those obtained using the even-even and odd-A nuclei alone.

For the levels above 500 keV the situation is less satisfactory, in particular with regard to the spins and parities. Our experimental knowledge on parities is limited to the results from the transfer reactions, and most spin assignments are only tentative. Our own assumptions on the parities for the higher-lying levels is solely based on the observation that the $E1$ transitions between the low-lying levels in ^{196}Au are highly hindered due to the very different two-quasiparticle structure predicted for the levels with different parities. It is therefore crucial that future experiments concentrate on the determination of the spins and parities of the levels up to excitation energies of approximately 1 MeV. Our data indicate that such information can possibly be obtained from careful measurements of in-beam $\gamma\gamma$ angular correlations in the (p,n) reaction. Also a study of the $(\vec{d},\alpha)$ reaction with improved statistics could provide definite spins and parities for more states.

ACKNOWLEDGMENTS

We would like to acknowledge the help of H. Balzer, S. Boehmsdorff, M. Dorthe, P. E. Garrett, J. Kern, H. Lehmann, S. Manannal, J. Manns, J. L. Schenker, and T. Weber during some of the many experiments. This work was supported by the Deutsche Forschungsgemeinschaft (Grant Nos. IIC4 Gr 894/2 and Gu 179/3), the Paul Scherrer Institute, the Swiss National Science Fund, and the U.S. Department of Energy under Grant Nos. DE-FG02-91ER-40609 and DE-FG02-88ER-40417.

[1] A. Arima and F. Iachello, Ann. Phys. (N.Y.) **99**, 253 (1976).
[2] F. Iachello, Phys. Rev. Lett. **44**, 772 (1980).
[3] P. Van Isacker, J. Jolie, K. Heyde, and A. Frank, Phys. Rev. Lett. **54**, 653 (1985).
[4] A.B. Balantekin and V. Paar, Phys. Rev. C **34**, 1917 (1986).
[5] J. Jolie, U. Mayerhofer, T. von Egidy, H. Hiller, J. Klora, H. Lindner, and H. Trieb, Phys. Rev. C **43**, R16 (1991).
[6] G. Rotbard, G. Berrier, M. Vergnes, S. Fortier, J. Kalifa, J.M. Maison, L. Rosier, J. Vernotte, P. Van Isacker, and J. Jolie, Phys. Rev. C **47**, 1921 (1993).
[7] A. Metz, J. Jolie, G. Graw, R. Hertenberger, J. Gröger, C. Günther, N. Warr, and Y. Eisermann, Phys. Rev. Lett. **83**, 1542 (1999).
[8] A. Metz, Ph.D. thesis, University of München, 1999.
[9] N. Warr, S. Drissi, P.E. Garrett, J. Jolie, J. Kern, S.J. Mannanal, J.-L. Schenker, and J.-P. Vorlet, Nucl. Phys. **A620**, 127 (1997).
[10] J. Jolie *et al.* (unpublished).
[11] J. Gröger, diploma thesis, University of Bonn, 1996.
[12] Zh. Chunmei, W. Gongqing, and T. Zhenlan, Nucl. Data Sheets **83**, 145 (1998).
[13] J. Gröger, Ph.D. thesis, University of Bonn, 2000.
[14] C.W. Beausang, C.J. Barton, M. Caprio, R.F. Casten, J.R. Cooper, R. Krücken, Benyuan Liu, J.R. Novak, Z. Wang, A.N. Wilson, N.V. Zamfir, A. Zilges, and M. Wilhelm, Nucl. Instrum. Methods Phys. Res. A (to be published).
[15] D.C. Radford, Nucl. Instrum. Methods Phys. Res. A **361**, 297 (1995).
[16] K.S. Krane, R.M. Steffen, and R.M. Wheeler, Nucl. Data Tables **11**, 351 (1973).
[17] T. Yamazaki, Nucl. Data Tables **3**, 1 (1967).
[18] V. Kölschbach, P. Schüler, K. Hardt, D. Rosendaal, C. Günther, K. Euler, R. Tölle, M. Marten-Tölle, and P. Zeyen, Nucl. Phys. **A439**, 189 (1985).
[19] G. Graw (private communication).
[20] P. Petkov, W. Andrejtscheff, S.J. Robinson, U. Mayerhofer, T.

von Egidy, S. Brant, V. Paar, and V. Lopac, Nucl. Phys. **A554**, 189 (1993).
[21] U. Mayerhofer, T. von Egidy, P. Durner, G. Hlawatsch, J. Klora, H. Lindner, S. Brant, H. Seyfarth, V. Paar, V. Lopac, J. Kopecky, D.D. Warner, R.E. Chrien, and S. Pospisil, Nucl. Phys. **A492**, 1 (1989).
[22] A.B. Balantekin, I. Bars, and F. Iachello, Nucl. Phys. **A370**, 284 (1981).
[23] P. Van Isacker, A. Frank, and Hong-Zhou Sun, Ann. Phys. (N.Y.) **157**, 183 (1984).
[24] J. Jolie and P.E. Garrett, Nucl. Phys. **A596**, 234 (1996).
[25] A. Metz, Y. Eisermann, A. Gollwitzer, R. Hertenberger, B.N. Valnion, G. Graw, and J. Jolie, Phys. Rev. C (to be published).
[26] D.D. Warner, in *Algebraic Approaches to Nuclear Structure*, edited by R.F. Casten (Harwood Academic, GmbH, Switzerland, 1993), Chap. 5.